Nano Research Energy

ISSN 2791-0091 (print); 2790-8119 (online)
https://doi.org/10.26599/NRE.2023.9120045

Review Article

# Towards high power density aqueous redox flow batteries

Mengqi Gao[1], Zhiyu Wang[1], Dao Gen Lek[1], and Qing Wang[1,2] (✉)

[1] *Department of Materials Science and Engineering, College of Design and Engineering, National University of Singapore, 117574, Singapore*
[2] *Institute of Materials Research and Engineering (IMRE), Agency for Science Technology and Research (A*STAR), 138632, Singapore*

**Received:** 23 October 2022 / **Revised:** 19 November 2022 / **Accepted:** 20 November 2022

## ABSTRACT

With the increasing penetration of renewable energy sources in the past decades, stationary energy storage technologies are critically desired for storing electricity generated by non-dispatchable energy sources to mitigate its impact on power grids. Redox flow batteries (RFBs) stand out among these technologies due to their salient features for large-scale energy storage. The primary obstacle to the successful industrialization and broad deployment of RFBs is now their high capital costs. A feasible route to cost reduction is to develop high-power RFBs, since the increase in power performance has a pronounced impact on the cost of RFB systems. In this review, an in-depth inspection of the power performance of RFBs is presented. Perspectives for the future development of high-power RFBs along with implementable strategies addressing both the intrinsic and extrinsic limiting factors are summarized, which are expected to provide useful references steering the further improvement in the power density of RFBs.

## KEYWORDS

redox flow batteries, power density, aqueous electrolytes, redox kinetics, polarizations

## 1 Introduction

"Carbon neutrality" has been in dire need to address global warming and the entailed environmental and societal challenges, thus over 140 countries have pledged to reduce carbon emissions by 2030 [1]. Driven largely by the strong needs and technology developments along with supportive policy environment, exploitations of renewable energy sources, such as solar and wind, have more rapidly grown in recent years than ever before. However, because of the fluctuation and unpredictability, high levels of power generation from these non-dispatchable energy sources becomes challenging when directly integrated into electric power grids, which may impose a large impact on the grids or result in curtailment [2]. Therefore, advanced electrical energy storage systems (ESS) are urgently demanded to buffer the temporal deviation in the supply of renewable energy [3]. Various mechanical and thermal energy storage systems as well as rechargeable batteries have been employed for large-scale electricity storage [4]. Zero-carbon clean energy and longer-duration seasonal electricity storage can be provided by these technologies, which also contribute to alleviating grid congestion, stemming renewable curtailment, and increasing energy resilience.

Among the diverse ESS, rechargeable batteries have garnered attention worldwide for grid-scale electrical energy storage in recent years. Li-ion batteries (LIBs), the most widely used technology, have higher energy density and lower self-discharge rate than other battery technologies. However, the expansion of LIB market and its large-scale deployment are crucially hampered by safety concerns and availability of electrode materials [5]. Redox flow batteries (RFBs) are thus emerging as one of the most viable options for grid-scale stationary energy storage [6]. Owing to the salient feature of decoupled energy storage and power generation, the capacity of RFBs depends on the dimension of electrolyte tank in which redox species are stored, while the output power is determined by the specification of the battery stacks. This endows RFBs with excellent operational flexibility and scalability for various application scenarios [7]. More importantly, the water-based electrolyte of aqueous redox flow batteries (ARFBs) also guarantees environmental benignity, low cost, and inherent safety.

However, given the relatively-low concentration of redox mediators in electrolytes and severe polarizations at high-current operation, RFBs have the inherent weaknesses of low energy density and power density [8, 9]. The energy density of RFBs is dictated by the electrolyte concentration and cell voltage, while the stored energy could be independently remedied by increasing the volume of electrolytes, as the footprint is of less priority for most stationary RFB installations. In contrast, the variables that affect power density are much more complicated, as they are associated with all the kinetic events taking place inside the cell stack. The unsatisfactory power density would inevitably lead to increased size and number of cell stacks [10], whose cost comprises a major portion of the total RFB system [11]. Presently, a critical obstacle to the successful



Address correspondence to msewq@nus.edu.sg

industrialization and broad deployment of RFBs is now their economic viability, for which the capital cost of RFB systems must be reduced to enable compelling value propositions in ESS markets. Obviously, one feasible route to cost reduction is to develop RFBs with higher power densities, so as to reduce the stack size and consequently the overall cost [12]. As shown in Fig. 1, the increase in cell power density has a pronounced impact on the cost of a commercially viable RFB system, and as a result, the sensitivity to component costs of the repeating parts decreases substantially [13].

All-vanadium flow battery (VFB), known as the most mature flow cell system, presents the most promising power ability among all types of RFBs [14]. Nevertheless, the prohibitive cost of the electrolytes and membranes, as well as the scarcity of vanadium resources restrict its potential in the gird-scale application. According to the U.S. Department of Energy (DOE), the targeted cost for RFBs (2023) is less than 150 $/KWh, driving the necessity to adopt chemistries other than VFBs because the vanadium electrolyte alone has approached this level without taking other components into account [15]. Moreover, even though the footprint of flow battery system is not critically considered for large-scale applications, an improved power performance of RFBs could open new avenues for applications in other emerging areas, such as the integration of ARFBs with electronic devices and robots [16].

In recent years, many studies have been carried out with different strategies to improve the power density of various RFBs. In particular, non-aqueous RFBs have sparked research interests due to their wide electrochemical window and enormous varieties of organic redox species. However, the low conductivity and ion mobility create intractable polarization losses and extra costs. Therefore, if the realistically anticipated endpoint is high-power performance, one may reasonably conclude that the aqueous path presently appears to be more appealing.

An in-depth look into the power performance of ARFBs covers a wide range of parameters, which can be primarily divided into two aspects in this review: intrinsic and extrinsic factors (Fig. 2). Additionally, some practicable strategies and constructive advancements corresponding to each aspect have been succinctly outlined. This review is expected to provide useful suggestions and practical methodologies for developing high power density RFB systems for grid-scale applications and beyond.

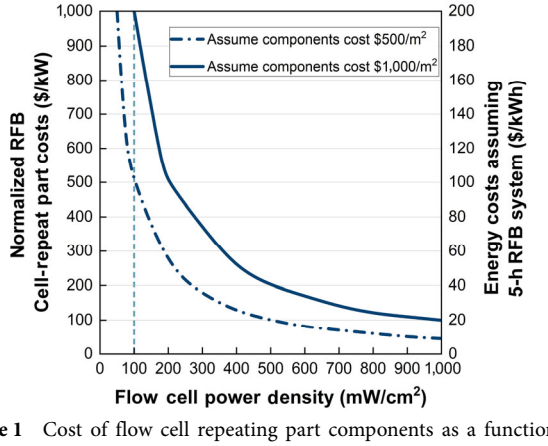


**Figure 1** Cost of flow cell repeating part components as a function of areal power density. The left axis is cost per power capability and the right axis is cost per energy, assuming a 5-hour discharge cycle. Redrawn with permission from Ref. [13], © The Electrochemical Society 2013.

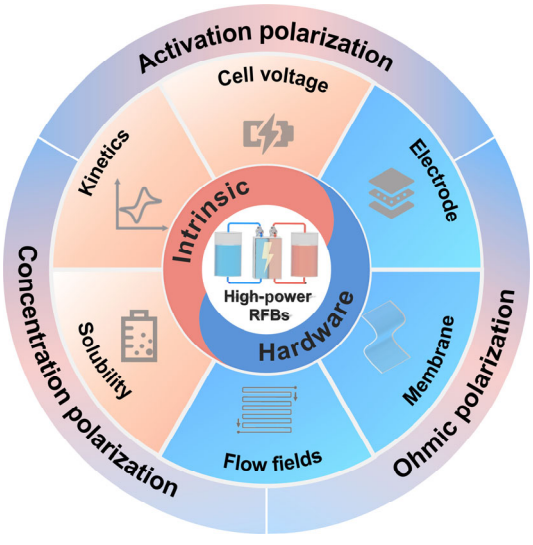


**Figure 2** The various factors that impact on the power performance of RFBs.

## 2 Crucial factors and strategies for improving the power density of RFBs

The power density or areal power stands for power per unit area that the battery can supply, which can be calculated by Eq. (1):

$$\text{Power density} = \frac{IV}{A}(\text{mW/cm}^2) \quad (1)$$

where $I$ is the discharge current, $V$ is the output voltage, and $A$ is the active electrode area of a flow cell. Therefore, maximizing the operating current density ($I/A$) whilst maintaining high voltage is necessary for improving power performance. However, the increased current density of a flow cell will inevitably aggravate the cell polarizations (or overpotentials), including activation polarization, ohmic polarization and concentration polarization, leading to impaired electrolyte utilization and output voltage [17]. Thus, these polarizations directly engender the loss of power and energy output. Figure 3 depicts the dominant sources of overpotentials derived from a generalized polarization curve [18]. It is acknowledged that polarizations are strongly affected by both intrinsic and extrinsic factors. For instance, ohmic polarization is mainly induced by the resistance of cell hardware, while activation polarization is attributed to the reaction kinetics of redox species at electrode/electrolyte interface, and concentration polarization results from diffusion limitation of redox species in electrolyte [19]. In this section, the foremost factors dictating the power performance of RFBs and strategies for improvement will be discussed in detail.

### 2.1 Redox mediators

The intrinsic factors, primarily associated with the electrochemical characteristics of the redox active materials, impact the power performance of RFBs via activation and concentration polarizations. The theoretical power and energy outputs of RFBs basically hinge on the intrinsic features of redox mediators due to their direct involvement in the electrochemical processes [20]. Herein, three crucial intrinsic features will be covered: reaction kinetics, cell voltage and charge concentration, which are directly related to the power output of RFBs.

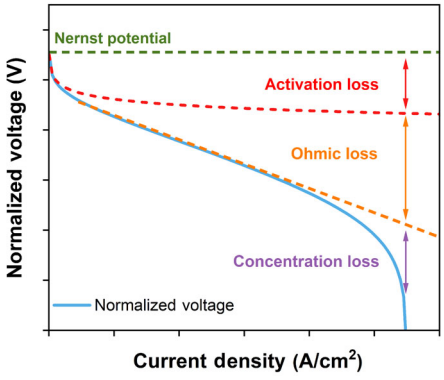


**Figure 3** Generalized polarization curve for a flow battery. The dominant sources of overpotential losses in each region are indicated.

### 2.1.1 *Electrochemical kinetics*

Electrochemical kinetics of redox mediators have a significant impact on RFB performance. An ideal RFB requires redox mediators with desirable redox potential, reversibility, and kinetics for the redox reactions. The heterogeneous electron transfer rate constant, embodied in $k^0$, is often used to assess the reaction kinetics of redox species. A high $k^0$ indicates a fast reaction and allows for high current densities that can be drawn from the cell without raising overpotentials, while low values of $k^0$ indicate sluggish kinetics that would necessitate a large overpotential to overcome [21]. Figure 4 depicts the simulated power densities of three batteries consisting of redox species with different rate constants, which shows the influence of reaction kinetics of the redox systems on the delivered power densities of RFBs. Various electrochemical techniques, such as cyclic voltammetry (CV) and linear sweep voltammetry (LSV) measurements have been used to determine $k^0$ and diffusion coefficient $D_0$ [22]. Herein, the $k^0$ values of some typical redox mediators in RFBs are listed in Table 1 [23–27].

Previous research mostly focused on the electrocatalysts to boost reaction kinetics, and most studies on this subject have been aimed at VFBs. The catholyte reaction ($VO^{2+}/VO_2^+$) in VFBs suffers from inherently slow reaction kinetics, which involves the transfer of an oxygen atom from $H_2O$ molecule to vanadium species in multiple steps. The $V^{2+}/V^{3+}$ reaction is even slower than the cathode side and negatively impacted by parasitic hydrogen evolution reaction (HER) [28]. To improve the activity of vanadium redox couples and suppress the parasitic reactions, additions of hybrid carbon nanomaterials

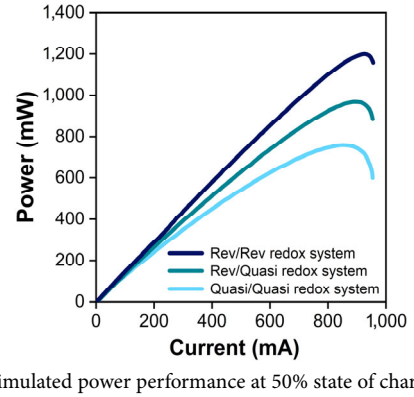


**Figure 4** Simulated power performance at 50% state of charge (SOC) for three RFBs of different combinations of reversible and quasi-reversible redox systems, with $k^0$ of $3\times10^{-1}$ and $2\times10^{-4}$ cm/s, respectively. Redrawn with permission from Ref. [22], © American Chemical Society 2020.

**Table 1** $k^0$ values of some typical redox mediators in RFBs

| Inorganic redox mediators | | | Organic redox mediators | | |
|---|---|---|---|---|---|
| | $k^0$ (cm/s) | pH | Derivatives | $k^0$ (cm/s) | pH |
| $V^{2+}/V^{3+}$ | $10^{-6}$–$10^{-4}$ | Acid | TEMPO-based | $10^{-3}$–$10^{-2}$ | Neutral |
| $VO^{2+}/VO_2^+$ | $10^{-6}$–$10^{-4}$ | Acid | Viologen-based | $10^{-3}$–$10^{-1}$ | Neutral |
| $Fe^{2+}/Fe^{3+}$ | $10^{-4}$–$10^{-3}$ | Acid | Quinone-based | $10^{-3}$–$10^{-2}$ | All pH |
| $Br^-/Br_2$ | $10^{-4}$–$10^{-2}$ | Neutral/ Acid | Ferrocene-based | $10^{-4}$–$10^{-2}$ | Neutral |
| $Ce^{3+}/Ce^{4+}$ | *c.a.*$10^{-3}$ | Acid | Phenazine & Phenothiazine-based | $10^{-3}$–$10^{-1}$ | Alkaline |
| $Fe(CN)_6^{3-/4-}$ | *c.a.*$10^{-1}$ | Neutral/ alkaline | | | |

Note: 1. The values of $k^0$ for inorganic species vary with different electrode substrate materials. 2. TEMPO refers to 2,2,6,6-Tetramethylpiperidine-1-oxyl.

(e.g., graphene oxide or carbon nanotubes), a variety of metals (Ir, Ru, Bi, etc.) and transition metal oxides ($IrO_2$, $Mn_3O_4$, $WO_3$, $PbO_2$,) have been proposed [29, 30]. For instance, Li et al. used bismuth as a catalyst to accelerate the reaction kinetics of $V^{2+}/V^{3+}$ while suppressing HER. The energy efficiency of the VFB with Bi increased by 11% at a current density of 150 mA/cm$^2$ (Fig. 5(a)), and the power density and energy density were highly enhanced as well [31]. In 2018, Zhang et al. proposed an unprecedented method based on redox-targeted catalysis to tackle the kinetics issue of VFBs [32]. Prussian blue (PB) and a Prussian blue analogue (PBA) with identical redox potentials to $VO^{2+}/VO_2^+$ and $V^{2+}/V^{3+}$ were grafted on cathode and anode, respectively. Upon operation, the reversible proton-coupled redox-targeting reactions between PB and $VO^{2+}/VO_2^+$ on the cathode, PBA and $V^{2+}/V^{3+}$ on the anode facilitated the interfacial charge transfer of the vanadium species and concomitantly inhibited the side reactions. This improved the selectivity of the redox reactions and considerably enhanced the round-trip energy efficiency in a wide range of current densities.

In addition to VFBs, polysulfide-based RFB is another promising energy storage system, while the polysulfide species also suffer from sluggish reaction kinetics. Studies have shown that transitional metals and metal sulfides could function as effective electrocatalysts for aqueous polysulfide reactions. Ma et al. introduced a $CoS_2$/CoS heterojunction as electrocatalysts for aqueous polysulfide/iodide RFB and achieved an energy efficiency of 84.5% at 10 mA/cm$^2$ and a power density of 86.2 mW/cm$^2$ (Fig. 5(b)) [33]. However, hydrothermal and hydrogen reduction methods are usually employed to synthesize the above catalysts on electrode substrates, which are costly and unsuitable for large-scale preparation. To overcome this drawback, Gao et al., employed the successive ionic layer adsorption and reaction (SILAR) technique to deposit copper sulfide (CuS) on electrode as a highly efficient catalyst for polysulfide electrolyte. SILAR method could be feasibly conducted at room temperature without a requirement for sophisticated apparatus, and the deposition could be easily controlled even for large-area substrates. With $[Fe(CN)_6]^{4-/3-}$ as catholyte and polysulfide as anolyte, the flow cell has attained a power density of 116 mW/cm$^2$ and an energy efficiency of 77.7% at 50 mA/cm$^2$ (Fig. 5(c)), markedly superior to the previous polysulfide-based RFBs [34].

Compared with the traditional inorganic redox couples, organic redox molecules generally exhibit superior reaction rate constants (See Table 1). Based on the structure-property

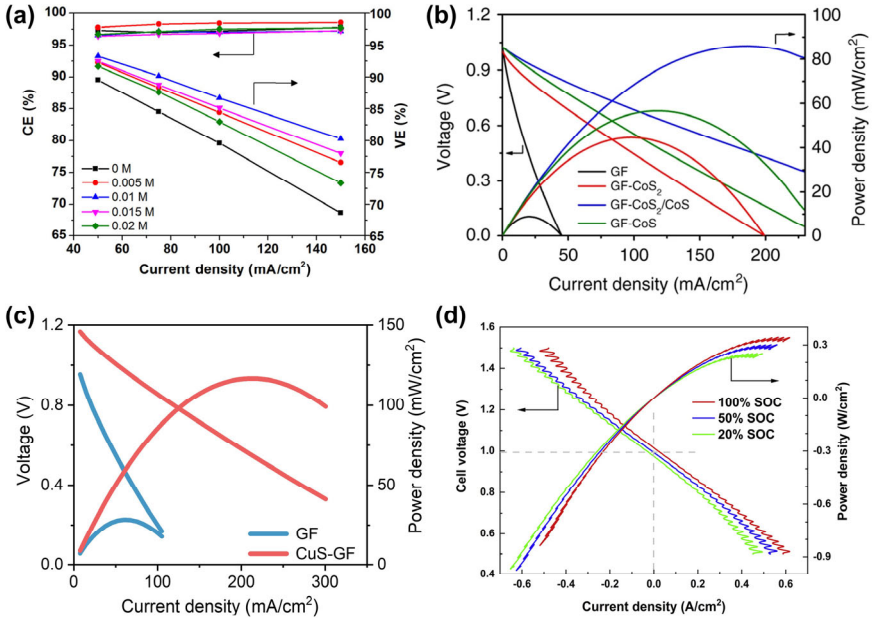


**Figure 5** (a) CE and VE performance of VFBs containing different $Bi^{3+}$ concentrations as a function of charge/discharge current density. Reproduced with permission from Ref. [31], © American Chemical Society 2013. (b) The discharge polarization and power density curves of the polysulfide-iodide RFBs with GF, GF-CoS2, GF-$CoS_2$/CoS, and GF-CoS electrodes at 50% SOC. Reproduced with permission from Ref. [33], © Ma, D. et al. 2019. (c) The discharge polarization and power density curves of the polysulfide-$[Fe(CN)_6]^{4-/3-}$ cells at 100% SOC when GF and CuS-GF were used as the negative electrode, respectively. Reproduced with permission from Ref. [34], © Elsevier Ltd. 2020. (d) 0.5 M DPivOHAQ/Ferrocyanide Full Cell at pH 12: Cell voltage versus current density at room temperature (~20 °C) at various SOC. Reproduced with permission from Ref. [36], © Elsevier Inc. 2020.

relationships, it has been reported that faster reaction kinetics of redox molecules could benefit from a narrower energy gap between the lowest unoccupied and highest occupied molecular orbital (LUMO and HOMO) [26, 35]. Meanwhile, the well-developed organic synthesis techniques have significantly promoted the development of novel organic electroactive species with desired properties. In 2020, 3-3'-(9,10-anthraquinone-diyl)bis(3-methylbutanoic acid) (DPivOHAQ) was proposed by Aziz's group to pair with a ferrocyanide catholyte [36]. Owing to the rapid redox reactions of both DPivOHAQ and ferrocyanide, the full cell delivered a peak power density of 340 mW/cm$^2$, despite the open-circuit voltage (OCV) was only 1.0 V (Fig. 5(d)), and a record-low capacity fade rate of <1% per year was demonstrated. The employment of organic active species liberates redox chemistries from the constraints of materials availability and opens up vast opportunities for searching viable redox active species for next-generation RFBs.

A comprehensive overview of different electrocatalysts for RFBs has been reported by Amini et al. [37]. It should be noted that the addition of catalysts increases the complexity and cost of electrode preparation, and practically it could be difficult to ensure a uniform distribution of the catalysts lasting for years of operation. As such, there is an urgent demand for cost-effective and reliable techniques to prepare catalysts in large scales. In addition to electrocatalysts, some other attempts have also been undertaken to promote the reaction kinetics of batteries. For instance, the use of additives into electrolyte has been reported to enhance the kinetics of vanadium reactions [38]. Additionally, the modification of electrode structure was also found to be effective in enhancing power performance, for which more details will be elaborated in Section 2.2.1. Lastly, it is envisaged that the development of advanced computational and synthetic methodology will accelerate the screening of organic redox alternatives with favorable redox kinetics.

### 2.1.2 *Cell voltage*

Obviously, expanding the cell voltage is of great significance for RFBs for it is beneficial to both the energy and power density. Figure 6(a) shows the simulated peak power densities of RFBs with different voltages. With the cell voltage increasing from 0.90 to 1.60 V, more than twice of the peak power density can be achieved. Towards a high cell voltage cell voltage, the separation of the redox potentials between anolyte and catholyte of a flow battery should be maximized, while they should be within the electrochemical stability window of the solvent. For aqueous electrolytes, the theoretical voltage window of water is 1.23 V, but in practice, the accessible voltage of ARFBs could be considerably wider considering the overpotentials for $H_2/O_2$ evolution on the electrodes [39]. More importantly, a wider potential window also allows for more candidates of redox species in RFBs.

To obtain a high cell voltage, a wide variety of redox mediators of both anolyte and catholyte have been examined. In 2022, Wang et al. reported a high-power ARFB using cerium sulfate ($Ce_2(SO_4)_3$) as catholyte and polyoxometalate (POM) as anolyte, which achieved an operating voltage of 1.85 V in acidic condition (Fig. 7(a)) [40]. The POM-Ce flow battery presented a power density of 1.40 W/cm$^2$, which was considerably higher than the VFB (0.89 W/cm$^2$) tested with the same setup (Fig. 7(b)), despite that the concentration of vanadium species was 15 times higher than POM-Ce cell. As the widest voltage window of aqueous electrolyte usually appears at a neutral pH [41], there have been several attempts to construct neutral-pH high voltage RFBs. In 2019, Robb et al. reported a chelated chromium ion $[Cr(PDTA)]^-$, offering a redox potential of –1.31 V vs. Ag/AgCl. With the ability to prevent water coordination and inhibit HER, $[Cr(PDTA)]^-$ was paired with $Fe(CN)^{3-/4-}$ in a near-neutral buffer electrolyte,

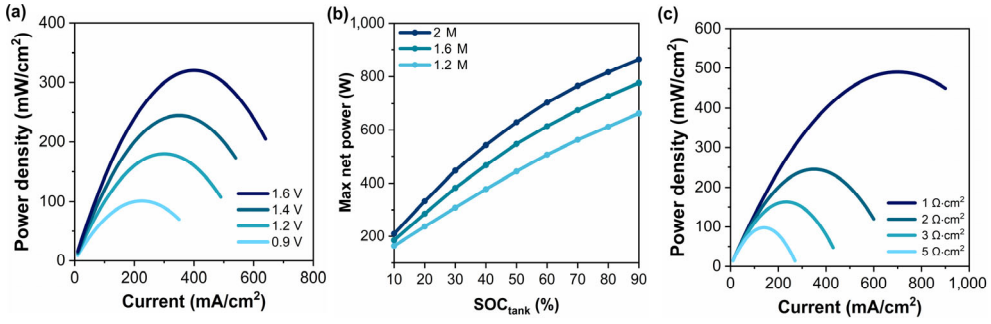


**Figure 6** Simulated power density for RFBs with different output voltage (0.90, 1.20, 1.40 and 1.60 V). The overall area specific resistance (ASR) of each battery is assumed to be 2 Ω·cm$^2$, without considering other voltage losses. (b) Physics-based model to predict maximum net power of VFBs, which controls inputs for SOC from 10 to 90% with different vanadium concentrations of 2.0, 1.6, and 1.2 M. Redrawn with permission from Ref. [47], © Elsevier B.V. 2014. (c) Simulated power density of RFBs with different overall ASR from 1–5 Ω·cm$^2$. OCV of each battery is assumed to be 1.40 V, without other voltage losses taken into condition.

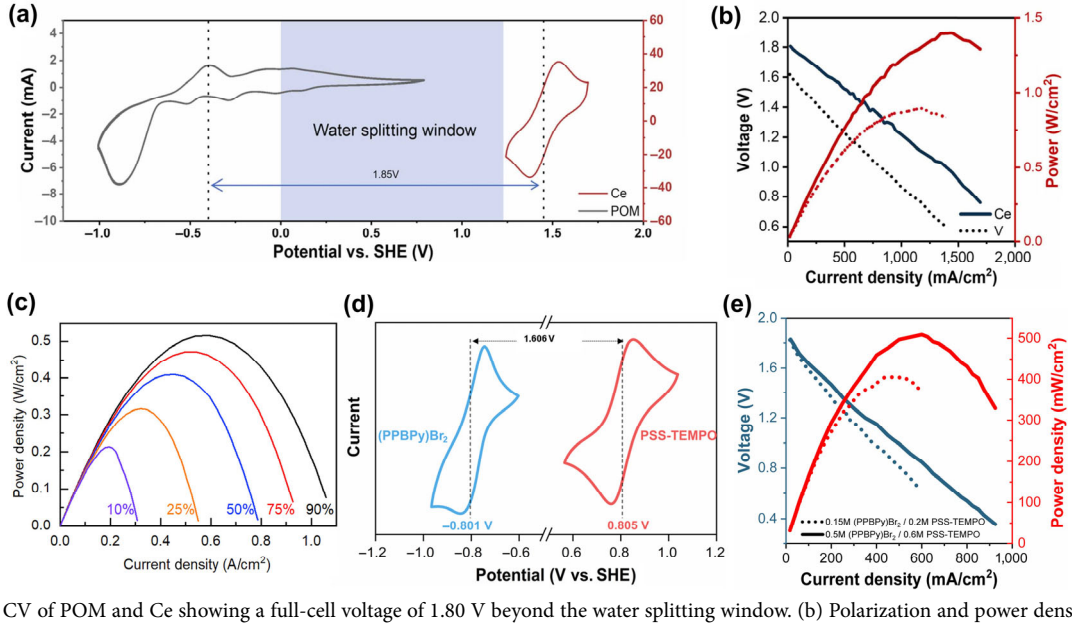


**Figure 7** (a) CV of POM and Ce showing a full-cell voltage of 1.80 V beyond the water splitting window. (b) Polarization and power density curves of a POM-Ce flow battery (70 mM POM + 65 mM cerium sulfate) employing Nafion 212 membrane and its comparison with a VFB (1.5 M). Reproduced with permission from Ref. [40], © Elsevier Ltd. 2021. (c) Power density versus current density at varying SOC of battery with 0.4 M CrPDTA in 0.2 M KBi vs. 2.0 M KBr and 0.5 M $Br_2$ in 0.1 M KBi. Reproduced with permission from Ref. [42], © Elsevier Inc. 2020. (d) CV curves of 20 mM (PPBPy)$Br_2$ (blue) and PSS-TEMPO (red) in 1 M NaCl. (e) Polarization curves and power densities of the two (PPBPy)$Br_2$/PSS-TEMPO flow cells at 100% SOC. Reproduced with permission from ref. [44], © Wiley-VCH GmbH 2022.

with which a voltage of 1.62 V could be achieved. A peak power density above 500 mW/cm$^2$ was thus revealed (Fig. 7(c)) [42]. Moreover, due to the diversity and structural tunability of organic molecules, some organic redox species have been designed by introducing specific functional groups to fully exploit the electrolyte potential window, and some strategies such as conjugation fusion or electron coupling have been proposed to design new organic redox molecules [43]. Recently, Gao et al. demonstrated an all-organic aqueous RFB with a TEMPO derivative as catholyte and a viologen derivative as anolyte, namely PSS-TEMPO and (PPBPy)$Br_2$, respectively (Fig. 7(d)) [44]. The assembled flow battery afforded a high cell voltage of 1.61 V and a peak power density of 509 mW/cm$^2$ (Fig. 7(e)), among the highest records in pH-neutral all-organic ARFBs. As previously indicated in Section 2.1.1, the redox organic molecules also have the advantage of fast reaction kinetics, thus it is anticipated that rigorous molecular engineering along with the aid of computational studies, will promote the exploration of organic electroactive species with desirable properties to meet the requirement for high-power RFBs.

As the onset potentials of OER and HER vary with pH, the electrochemical stability window can be deliberately adjusted to accommodate the redox mediators with even more positive or negative redox potentials by regulating electrolyte pH. A three-electrolyte, two-membrane configuration has been proposed accordingly, where both alkaline and acidic electrolytes are utilized and separated by a neutral electrolyte chamber. The neutral electrolyte chamber is encapsulated by two membranes (one AEM and the other CEM) with ion selectivity on each side. Through this setup, high voltage Zn-$MnO_2$ (2.83 V) and Zn-Ce (3.08 V) hybrid flow batteries have been reported [45, 46]. However, there is an issue regarding this setup: the $OH^-$ and $H^+$ in negative and positive electrolytes would migrate to the middle compartment, where an acid-base neutralization reaction occurs irreversibly, resulting in a decreased concentration of acid and alkaline and impairing the battery performance and stability. Moreover, the employment

of both AEM and CEM will also increase the internal resistance and ohmic polarization, which may offset the advantage of high cell voltage.

To sum up the above discussion, there have been multiple attempts to construct high-voltage ARFBs by employing suitable redox mediators, with which substantially high power and energy outputs have been achieved. Additionally, some adjustments of supporting electrolytes have also been proposed to widen the electrochemical stability window of aqueous electrolytes, which will be further discussed in Section 2.2.2. It should be underlined there will always be side reactions (HER and OER) if the pH across the catholyte and anolyte is the same and the cell voltage is higher than 1.23 V. Considering the long-term operation in a practical scenario, the traces of side reactions may gradually alter the pH of electrolyte solution and induce stability problem.

### 2.1.3 *Charge concentration*

In addition to redox potential, the concentration of redox couples in electrolytes is another decisive parameter for the overall performance of RFBs. Considering the multiple electron transfer of some redox mediators and some specific methods to improve the maximum number of active species stored per unit volume (such as semi-solid, redox-targeting, etc.), the term "effective concentration of charges" in this context would be more precise instead of "concentration of redox species". The elevated charge concentration is not only beneficial to energy density but also advantageous for enhancing the maximum current density that can be withdrawn from the cell without provoking reactant depletion and voltage losses, leading to superior power performance (Fig. 6(b)) [47]. There are several strategies to increase the charge concentration in RFBs: (1) Select the redox species with high solubility or multiple electron transfer; (2) Modify the existing species to boost the solubility, usually more applicable for organic redox molecules; (3) Construct metal-hybrid or semi-solid RFBs; (4) Employ redox-targeting (RT) based RFBs.

Various redox couples have been investigated over the past few decades, among which aqueous polysulfide species has a theoretical volumetric capacity as high as 353.8 Ah/L resulting from 2-electron transfer and high solubility (>8 M). Furthermore, given the high solubility of polyhalide materials, the polysulfide-polyhalide based RFBs have received particular attention in recent years. A polysulfide-iodide RFB was demonstrated by Li et al. [48] with a much lower chemical cost ($85.4/kWh) and a higher energy density of 43.1 Wh/L than VFBs ($150/kWh, 25 Wh/L) (Figs. 8(a) and 8(b)). Apart from the redox materials with intrinsically high solubility, molecular engineering provides an effective way of enhancing the solubility and electron transfer properties of organic molecules. The grafting of highly hydrophilic functional groups, such as ammonium, sulfonate, carboxylate, and phosphate groups, has been extensively reported as an efficient strategy to improve the water solubility of hydrophobic organic/ organometallic compounds [3, 49]. For instance, ferrocene is nearly insoluble in water, but through the above design principle and synthetic strategy, the solubility can be boosted up to 2–4 M in water and as such various ferrocene derivatives have been utilized in ARFBs [50, 51]. Similar strategies have also been applied to anthraquinone derivatives. Aziz's group reported a water-miscible molecule, AQ-1,8-3E-OH (Fig. 8(c)), which enabled a volumetric capacity of 80.4 Ah/L at 1.5 M concentration. Pairing with ferrocyanide, the flow cell presented an energy density of 25.2 Wh/L and a power density of 170 mW/cm$^2$ at a neutral pH (Fig. 8(d)) [52]. More recently, eutectic electrolyte has also been reported as a novel strategy to enhance the energy density of RFBs as they offer advantageous features such as low cost, ease of preparation, and high concentration of active materials [53, 54].

To elevate the effective electron concentration, hybrid and semi-solid RFBs have also been extensively investigated recently. In hybrid RFBs, at least one of the active species is in solid form (e.g., Fe, Zn, $MnO_2$) on the electrode [55]. The active species are electrodeposited on the electrode surface during charging (Fig. 9(a)), and dissolve again during discharging. This configuration is expected to yield a higher energy density than the soluble redox mediators (while not always the case if the soluble form of the active species has limited solubility). Zinc-based RFB is the best-known example [56, 57], and

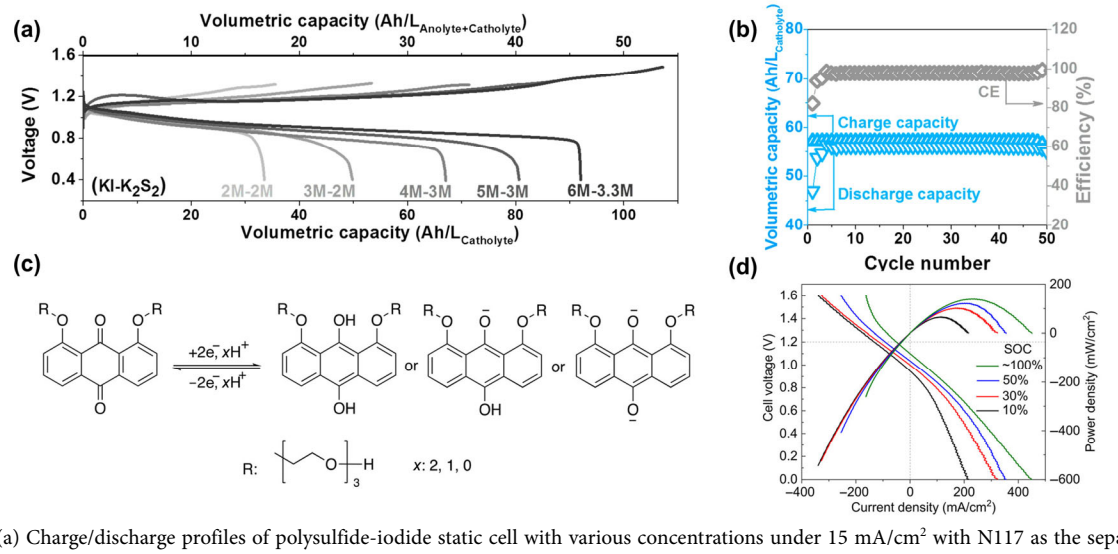


**Figure 8** (a) Charge/discharge profiles of polysulfide-iodide static cell with various concentrations under 15 mA/cm$^2$ with N117 as the separator (SOC 100%). (b) Cycling retention in coulombic efficiency and volumetric capacity of polysulfide-iodide static cell (3.0 M $K_2S_2$–4.0 M KI). Reproduced with permission from Ref. [48], © Elsevier Ltd. 2016. (c) Molecular structure of AQ-1,8-3E-OH and three different reduction products related to pH. (d) Cell voltage and power density versus current density at different SOC. Electrolytes comprised 1.5 M AQ-1,8-3E-OH anolyte and excess potassium ferro/ferricyanide catholyte. Reproduced with permission from Ref. [52], © American Chemical Society 2019.

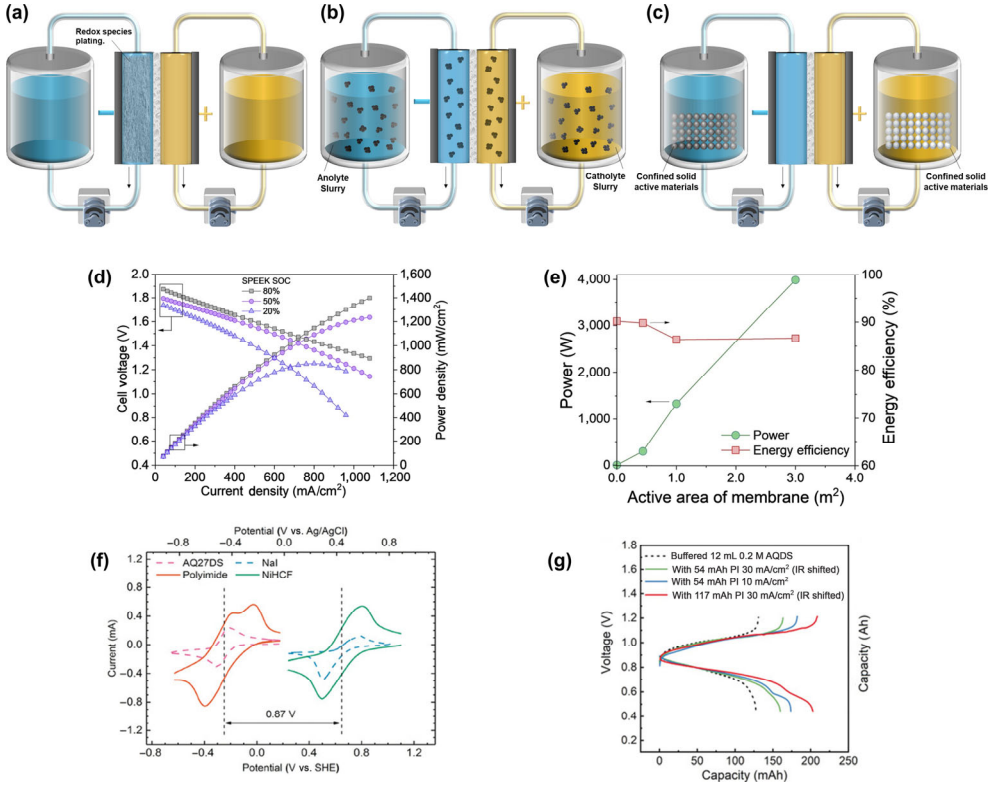


**Figure 9** Schematic diagrams for the configurations of (a) hybrid RFBs (b) semi-solid RFBs and (c) redox-targeting based RFBs. (d) The polarization curves of the alkaline zinc-iron RFB at different SOC using SPEEK membrane. (e) Power and energy efficiency of zinc-iron RFB stacks of different areas. Reproduced with permission from Ref. [58], © Elsevier Inc. 2022. (f) CV curves of polyimide (PI)/2,7-AQDS and nickel hexacyanoferrate (NiHCF)/NaI. (g) Voltage profiles of buffered 0.20 M 2,7-AQDS/NaI full cell after adding PI solid materials. Reproduced with permission from Ref. [64], © Wiley-VCH Verlag GmbH & Co. KGaA, Weinheim. 2020.

various configurations have been proposed including Zn-Br, Zn-I and Zn-Fe, etc. In 2022, Li's Group achieved a power density of 1.4 W/cm$^2$ with an alkaline zinc-iron RFB (Figs. 9(d) and 9(e)), for which superior performance has been accomplished from lab-scale to kW-scale stacks using a homemade SPEEK membrane [58]. However, the dendrite formation could become a pressing challenge when large quantities of zinc are deposited [59], and the non-uniform plating and stripping may cause a disparity in capacity among the individual cells. In addition, since the plating and de-plating of active species are limited by the size of electrode, one of the key features of RFBs, namely, decoupling of power and capacity is compromised in the hybrid systems. As for semi-solid RFBs, the solid active compounds (e.g., $LiFePO_4$, $LiCoO_2$) and conducting additives are well mixed into a slurry to form electrolytes (Fig. 9(b)), with which a high equivalent charge concentration up to 10–40 M can be reached [60]. However, the power performance is formidably impeded by the high viscosity and low electronic conductivity of the mixture. And the presence of a large quantity of solid materials in the slurry produces complex fluid dynamics, thereby compromising energy efficiency and imposing challenges in maintenance [61–63].

Another approach that breaks the boundary between liquid and solid energy storage is redox targeting-based flow batteries (RTFBs). Within RTFBs, the redox mediators firstly receive electrons or holes from the electrode via a conventional electrochemical process, and then chemically react with the solid materials that are confined in electrolyte tanks [65–67]. The redox mediators are then regenerated on the electrode through the electrolyte flow for the next round of reaction (Fig. 9(c)). With such RT reactions, the solid battery materials are physically liberated from the electrode and could be placed in electrolyte tanks, enabling the system to only circulate electrolyte with dissolved redox mediators at a moderate concentration, while the energy density of RTFBs can in theory be as high as those with energy stored in electrode sheets with an enclosed battery configuration [63]. Meanwhile, the solid materials can stabilize the SOC changes of redox mediators, which is favorable to maintaining a high-power output during battery operation (Fig. 6(b)). In 2020, Zhou et al. reported a polyimide (PI, –0.27 V and –0.21 V vs. SHE) material as the capacity booster for AQDS (–0.25 V vs. SHE) in pH-neutral conditions [64]. The capacity of AQDS anolyte was boosted to 97 Ah/L at 30 mA/cm$^2$ with a solid material utilization as high as 83%. Combined with NaI-based catholyte and nickel hexacyanoferrate as the catholyte capacity booster, a full cell energy density of 39 Wh/L has been achieved (Figs. 9(f) and 9(g)). In RTFBs, the utilization of solid materials may become constrained by the RT reaction kinetics, especially at high current densities. The two-molecule RT systems, while they have a larger room for adjusting the driving force of interfacial charge transfer, have a compromised voltage efficiency. In single-molecule RT (SMRT) systems, due to the slanting voltage profiles of some solid materials and the resulting mismatch of redox potentials, only a fraction of the capacity could be utilized by SMRT reactions, which results in a reduced material utilization.

In brief, to raise the charge concentration of RFBs, modifying the functional groups and structures of the robust organic

species is expected to be effective approach to further improve the solubility and number of electrons stored. Meanwhile, RTFBs have shown great promise in significantly boosting the energy density and power performance. Due to the critical requirement for potential matching, the choices of redox mediators with good stability and fast reaction kinetics are seemingly limited. It is thus vital to search for highly dynamic redox mediator and charge storage material pairs that have rapid kinetics and matched potentials. Ingenious molecular engineering and highly customizable organic redox species open a plethora of new opportunities for searching suitable redox active materials.

## 2.2 Battery hardware and operating conditions

While a multitude of chemistries and reaction processes of RFBs have been extensively studied in the community, the path to the upscaling of RFBs has always been challenging and lack of adequate studies. For industrial applications, the full potential of RFBs has yet to be achieved, and the practically attainable energy and power outputs may be considerably lower than the theoretical values due to the severe polarizations at high-current-density operation [68], which results in higher cell stack costs and decreased single-pass energy conversion rates. For instance, Fig. 6(c) illustrates the profound impact of ohmic polarization on the power performance: when the overall ASR of a flow cell increases from 1 to 5 $\Omega \cdot cm^2$, the simulated power density sharply declines from 500 to 100 $mW/cm^2$ (assumed an OCV of 1.40 V). The optimization of hardware design, particularly related to ohmic and concentration polarizations, has become crucial to develop high-performing and commercially competitive RFBs. Moreover, the operation conditions, such as flow rate and working temperature, have also been identified as important factors. It has been commonly acknowledged that power performance can be improved at an elevated temperature due to the enhanced kinetics, however, there may be stability issue for some redox species at high temperature, especially for VFBs. Thus, the exploration of high performance RFBs at low working temperature is also an intriguing topic [69].

In this section, the strategies pertinent to the electrode, membrane and supporting electrolyte will be examined, along with the various flow field architectures that will be introduced from an engineering perspective.

### *2.2.1 Electrode*

Electrode is one of the core components of RFBs, supplying active reaction sites for the dissolved redox species upon charging/discharging. The performance of electrode is associated with activation, ohmic and concentration polarizations upon operation. An ideal electrode for RFBs should possess high electrochemical activity, high conductivity, low resistance for mass transport, excellent mechanical, thermal and chemical stability [70]. Carbon materials, particularly carbon felts (CFs) and graphite felts (GFs), are frequently employed as electrodes owing to their eminent three-dimensional porous structures and high specific areas. These features can minimize concentration polarization and activation polarization by providing unhindered mass transport for electrolytes and sufficient active reaction sites for redox species [19]. However, carbon-based electrodes are typically plagued by issues such as their hydrophobic nature and poor electrochemical activity. As the different types of polarizations are generally induced by multiple factors, the effects of different strategies are correlated and collective for the electrode performance [14]. Since the introduction of electrocatalyst has already been covered in Section 2.1.1, the following discussion will concentrate on the advancements in carbonaceous electrodes that have been made to enhance the electrochemical activity, conductivity, and wettability in aqueous RFBs.

Thermal activation, nitrogenization treatment, chemical treatment, electrochemical oxidation and doping have been extensively investigated as effective methods to improve the performance of carbon-based electrodes [71]. For instance, to improve the energy efficiency of VFBs, the pre-processing of GFs routinely includes heat and chemical treatment (e.g., $H_2SO_4$, $HNO_3$). The reinforced performance has been initially attributed to the formation of oxygen functional groups (C-O-H and C=O groups) on the electrode surface, which act as active sites to catalyze the electrochemical reactions (Figs. 10(a) and 10(b)) [72, 73]. Similarly, the introduction of nitrogen-containing groups by hydrothermal ammoniated treatment has been proposed to promote the kinetics and reversibility of $VO^{2+}/VO^{2+}$ and $V^{2+}/V^{3+}$ redox reactions [74, 75]. Although the pretreatment of carbon electrodes generally results in improved performance, the actual underlying mechanisms remain unclear, given that the incorporation of functional groups on the electrode surface not only increases the number of active reaction sites, but also greatly improves hydrophilicity and the affinity for redox species. Moreover, the surface modification of carbon electrodes should be redox-chemistry specific, as different redox reactions may have dissimilar requirements. For instance, it is suggested that the reductive treatment could accelerate the $VO^{2+}/VO^{2+}$ redox reaction, while the $V^{2+}/V^{3+}$ redox pair would prefer an oxidized surface treatment for electrodes [76].

The resistance of electrodes, bipolar plates, electrolytes, membrane, as well as the contact resistance between these components, are major contributors to the ohmic polarization of RFBs. For electrodes, ohmic polarization is largely derived from the material resistance associated with various geometric factors (i.e., area, thickness, porosity, tortuosity, etc.) as well as insufficient electrolyte diffusivity. Carbon-based electrodes could have their pore structures optimized by proper compression, which effectively improves the electrical conductivity, mass diffusion uniformity and mechanical stability. It is noteworthy that a number of variables, including the elastic modulus, thickness, clamping force, electrolyte flow pressure, etc., affect the compression ratio of carbon electrodes. Specifically, compared with carbon papers or cloths, carbon felts can usually withstand a higher compression ratio. The relationship between electrode compression ratio and battery performance has been the subject of several prior studies, and for carbon felts an optimal compression range of 20%–40% has been suggested [77, 78]. Beyond a certain compression range, the beneficial effect of reduced ohmic resistance would however be nullified by the high pressure drop and the loss of electrolyte permeability (Fig. 10(c)) [79].

In addition to carbon-based electrodes, some metallic electrodes (i.e. Ti, Ni, etc.) have been reported to have good electrochemical stability and catalytic property to facilitate the desired reactions, or high overpotentials for gas evolution to avoid side reactions [70]. It is, however, almost impractical to employ metallic electrodes in large scale due to high cost, corrosion, passivation, and low surface area. Other carbon-based materials, such as carbon paper and cloth, have attracted considerable interests within the community in recent years.

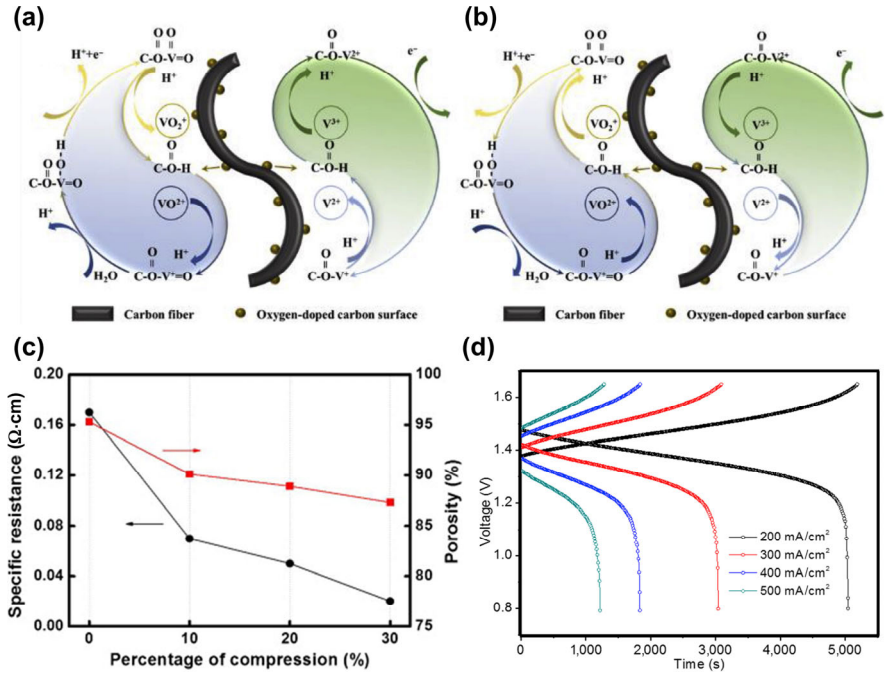


**Figure 10** (a) and (b) Schematic illustration of the reaction mechanisms of VFBs on the surface of oxygen doped electrode during charge and discharge. Reproduced with permission from Ref. [73], © Elsevier B.V. 2020. (c) Specific resistance and porosity vs. percentage of compression for FA-30A carbon felt electrodes. Reproduced with permission from Ref. [78], © Elsevier Ltd. 2014. (d) Charge-discharge curves of VRFBs with DPCE-1 carbon paper electrodes at the current densities of 200–500 mA/cm$^2$. Reproduced with permission from Ref. [80], © Elsevier B.V. 2016.

It has been reported that a dramatic increase of current and power density could be achieved by using carbon paper electrodes (Fig. 10(d)) [80], benefiting from their exceptionally low areal resistance [81], but the poor mechanical stability has become a serious impediment to widespread usage.

To date, a series of carbon materials are available for RFBs enabling a current density up to 600 mA/cm$^2$ [82]. Further enhancements in electrode activity could contribute to better power and energy performance with a higher operation current, allowing for a reduction in stack size. Meanwhile, a deeper comprehension of the fundamental kinetics processes is desired for the development of electrodes with superior performance. More practically, it should also be emphasized that the performances of commercial carbon-based electrodes vary significantly due to the different processing procedures and precursors. For instance, the bulk density of carbon felts may vary among brands and models by 0.03−0.05 g/cm$^3$, which impacts the compressibility and pre-treatment procedure, but is usually overlooked. Thus, when assessing the electrochemical performance, the source of electrode materials should also be taken into consideration.

### 2.2.2 *Membrane and supporting electrolyte*

During the operation of RFBs, ion-exchange membrane (IEM) acts as a separator to prevent the cross-mixing of redox species in the catholyte and anolyte, while still allowing the passage of ionic charge carriers. The resistance of membrane accounts for a major contribution to the overall ohmic polarization. More importantly, the expensive IEMs usually represent one of the largest portion of the battery stack cost [11]. The optimization of IEMs thus becomes highly desired. An ideal membrane should have high ionic conductivity and selectivity, adequate stability, as well as a high ion-exchange capacity (IEC). The commonly used polymer-based IEMs in aqueous RFBs can be classified as cation-exchange membranes (CEMs) and anion-exchange membranes (AEMs). In acidic and neutral pH electrolytes, the resistance of AEMs tends to be higher than that of CEMs [83], while the stability of AEMs is even poor in alkaline conditions [84]. As a result, the power performance of RFBs using AEMs is generally not on par with those using CEMs [85]. As the historical development of IEMs for flow batteries has already been well reviewed elsewhere [86, 87], this section will cover the recent advancement of IEMs with the purpose of improving the power capability of RFBs.

The most popular CEM used in ARFBs, Nafion, is commercially available in different thicknesses. In general, a thinner membrane is more favorable for power density and energy efficiency due to its lower ionic resistance. However, the reduced thickness also results in a lower ionic selectivity, leading to the issue of redox species crossover (thus a lower coulombic efficiency). Therefore, there is a trade-off between high conductivity and high selectivity, yet both are desirable properties for IEMs. In order to improve the overall performance, Nafion has been modified into different composite membranes using inorganic and organic materials such as graphene oxide (GO) [88], $SiO_2$ [89], $TiO_2$ [90], polyvinylidene fluoride (PVDF) [91], etc. Proper pre-treatment processes have also proven to be a valid way to enhance the membrane performance [92–94]. Meanwhile, great efforts have also been made to develop alternative low-cost membranes. In 2021, Chen et al. designed and fabricated a pyridine-modified polybenzimidazole membrane (B-PBI) for VFBs (Fig. 11(a)) [95]. A VFB with B-PBI membrane exhibited a CE of 99.16% and a VE of 88.86% at 80 mA/cm$^2$ (Fig. 11(b)), which was superior to that with Nafion 115 (CE of 95.13%, VE of 87.05%). In addition, a poly ether sulfone/sulfonated polyether ether ketone (PES/SPEEK) membrane was reported for the alkaline zinc-iron RFBs, which revealed an average EE of 91.92% at

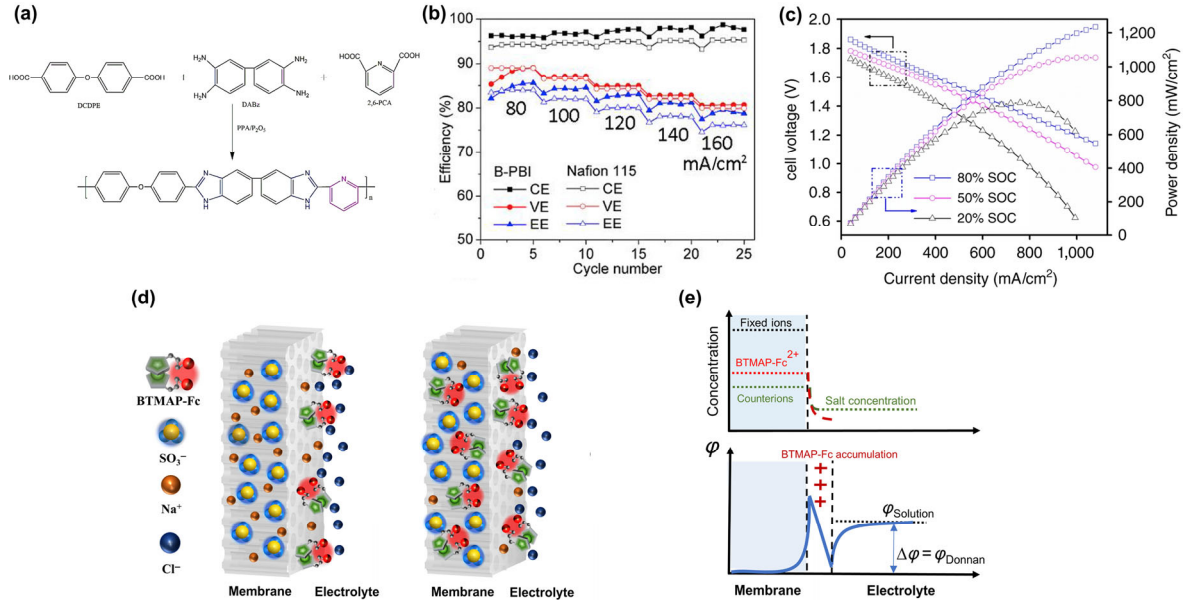


**Figure 11** (a) Synthesis route of B-PBI polymers. (b) VFB performance assembled with B-PBI and Nafion 115 membranes at various current densities. Reproduced with permission from Ref. [95], © Elsevier B.V. 2019. (c) The polarization of the alkaline zinc–iron flow battery at 80%, 50%, and 20% SOC using a PES/SPEEK membrane. The SPEEK content in the polymer is 20 wt.%. Reproduced with permission from Ref. [96], © Yuan, Z. et al. 2019. (d) Schematic illustrations of Nafion membrane and one-side interface just soaked in BTMAP-Fc electrolyte solution (left) and that after getting fouled (right). (e) Schematic drawing of the concentration profiles of various ionic species, and the potential changes across the membrane, electrolyte phase and the interface. The surface accumulated BTMAP-Fc results in an exclusion of $Na^+$ from transporting across the interface and through the membrane. Reproduced with permission from Ref. [97], © Elsevier B.V. 2022.

40 mA/cm$^2$, as well as a peak power density of 1.056 W/cm$^2$ (Fig. 11(c)) [96]. Apart from the properties of membranes, membrane fouling has frequently been observed to have profound impact on RFBs performance. Recently, Gao et al. conducted a systematic study of the membrane fouling phenomenon in aqueous RFBs [97]. It was demonstrated that the redox species possessing the same charge as the counterions of IEMs would accumulate inside the membrane and at the interface (Figs. 11(d) and 11(e)), blocking the ion-exchange sites and more critically creating an electric field at the interface excluding ion transport, which significantly deteriorated the power density and energy efficiency of RFBs. Thus, the appropriate selection of IEMs for RFBs becomes important to ensure a decent performance.

With regards to the supporting electrolytes, their properties have considerable impact on electrochemical stability window, membrane conductivity, and water migration between anolyte and catholyte. For different cations, the ion diffusion coefficient and conductivity in Nafion membrane increase in a sequence of $K^+ < Na^+ \approx Li^+ \ll H^+$ [98, 99]. As a result, the RFBs with acidic electrolytes (proton as charge carrier) usually deliver a high-power output largely due to the reduced ohmic polarization. As discussed in Section 2.1.2, cell voltage is generally limited by the electrochemical stability window of electrolyte. The widest voltage range is usually attained at a pH-neutral supporting electrolyte, and the types of electrolyte salts also have an influence on the electrochemical window, albeit petty [100]. Additionally, another effective approach to expanding the voltage of ARFBs is to increase the concentration of the supporting salt, as a lower water concentration would lead to a reduction in water activity [41]. Suo et al. proposed the idea of "water-in-salt" electrolyte, which was realized by dissolving ultra-soluble salts into water to obtain solutions containing more salt than water in both volume and weight ratio [101]. The "water-in-salt" electrolyte prevents water from directly interacting with the electrode materials due to the absence of free water molecules, resulting in a stable voltage window as wide as 3.0 V. Moreover, water migration across the membrane is another prevalent issue in many ARFBs, which causes a shift in concentration of redox species and increases the maintenance requirements. As the water transport through IEMs could be carried via the hydration shell of charge carriers, or driven by the osmotic pressure gradient, maintaining a balance of supporting electrolytes between anolyte and catholyte has emerged as a key to solving this issue. Also, the supporting electrolyte plays a vital role in some specific RFBs. For example, the poor solubility and weak thermal stability of vanadium ions in $H_2SO_4$ are well-known challenges for VFBs. The utilization of mixed acids as supporting electrolyte has been proposed as a useful method to enhance the solubility of vanadium species and extend the operation temperature range of VFBs [38].

In this section, the most influential features of membrane and supporting electrolyte are discussed. To date, most modifications of membranes have been targeted to fulfill the best possible balance between selectivity and conductivity, for retaining high coulombic efficiency and decreasing voltage loss. Energy efficiency and power density can thus be accordingly enhanced. The supporting electrolyte, affects the ionic conductivity and operation longevity, hence should be prepared carefully. Moreover, although the concentrated electrolyte has been frequently reported to widen the voltage window, the increase in viscosity and cost should be taken into consideration especially for large-scale applications.

### 2.2.3 *Flow fields and flow rate*

Multitudes of chemistries, including organic and inorganic

species, have been extensively investigated for RFBs in recent years. The architecture of RFBs, however, has remained nearly unchanged: porous electrodes are pressed against a graphite plate in most cell designs. Regarding the electrolyte transport, the uniformity of flow distributions within electrodes determines the concentration polarization and consequently affects cell performance. Non-uniform flow distributions imply that part of the electrodes is less effectively utilized, leading to an inflation of polarization and a loss in achievable power density and cell efficiencies. In the worst scenario, "dead" zones (areas with no reactants) occur within a large-size porous electrode [102]. Hence, the engineering design of flow field patterns and the optimization of flow rates become essential to maintain the same level of performance for upscaled RFBs.

Rapid and uniform electrolyte flowing through the electrode is a pivotal aspect to enhance the mass transport and minimize the voltage losses. Available strategies have been put forth involving designing rational battery configurations and flow fields on the electrode surface to optimize the electrolyte distributions. In 2012, Zawodzinski's group first reported a VFB with a "zero-gap" configuration, similar to that used in fuel cells (Fig. 12(a)) [81]. Electrolyte was delivered to the electrode via flow channels machined into the bipolar plates ("flow-by" configuration). Multiple times higher limiting current density and peak power density were demonstrated compared to the traditional "flow-through" configuration. Because the forced-convection occurs in porous electrodes in a flow-through geometry, the reactants and products are easily transferred, but relatively thick electrodes are usually required to reduce the pressure drop, posing a large ohmic loss. In contrast, the pressure drop can be reduced when flow-by channels are placed adjacent to the electrodes (Fig. 12(b)). For instance, serpentine flow field (SFF) has been introduced to produce the forced convection without severe pressure drop and reduce the electrode thickness. Another optimal design of flow-by configuration is interdigitated flow field (IFF), which allows electrolytes to flow in the electrodes perpendicular to the channels with forced convection (Fig. 12(c)). The pressure drop at IFF is higher than that of SFF, but less than that of flow-through ones. So far, there is still no consensus on the best flow channel design [102], while various studies on high performance RFBs employing flow fields have been reported, where the peak power density can reach around 2.6 W/cm$^2$ for VFBs [82, 103]. Over the past two decades, there has been a proliferation of issued patents on flow fields, bipolar plates and stacks used in flow batteries. However, it must be pointed out that before there is a simple and low-cost engraving technique to prepare customized flow channels on the bipolar plates, it does not seem viable to implement the flow-by configurations in grid-scale practical applications.

With regards to the role of flow rate in RFBs, increasing the flow rate of electrolytes is considered to be operative to decrease the concentration polarization and eliminate the "dead" zones, contributing to higher energy efficiency and power density [18]. In 2017, Marschewski et al. proposed a tapered-IFF design to enhance mass transport, and the imperative influence of electrolyte flow rate has been verified by a $K_4Fe(CN)_6$/2,6-dihydroxyanthraquinone (2,6-DHAQ) flow cell [104]. When the flow rate increased from 50 to 400 mL/min, the power density was boosted from 1,000 to about 1,400 mW/cm$^2$ (Fig. 13(a)). However, considering the increased pump loss, the highest net power density was attained at flow rates of 50–100 mL/min for 1 cm$^2$ active area (Fig. 13(b)). Therefore, trade-offs must be made between achieving the best flow distributions and minimizing pump losses. Furthermore, since direct monitoring of the flow distributions within RFBs is not experimentally accessible, multi-scale models and simulations have been employed as useful tools to assist understanding the complex mass transport, which could serve as valuable references for

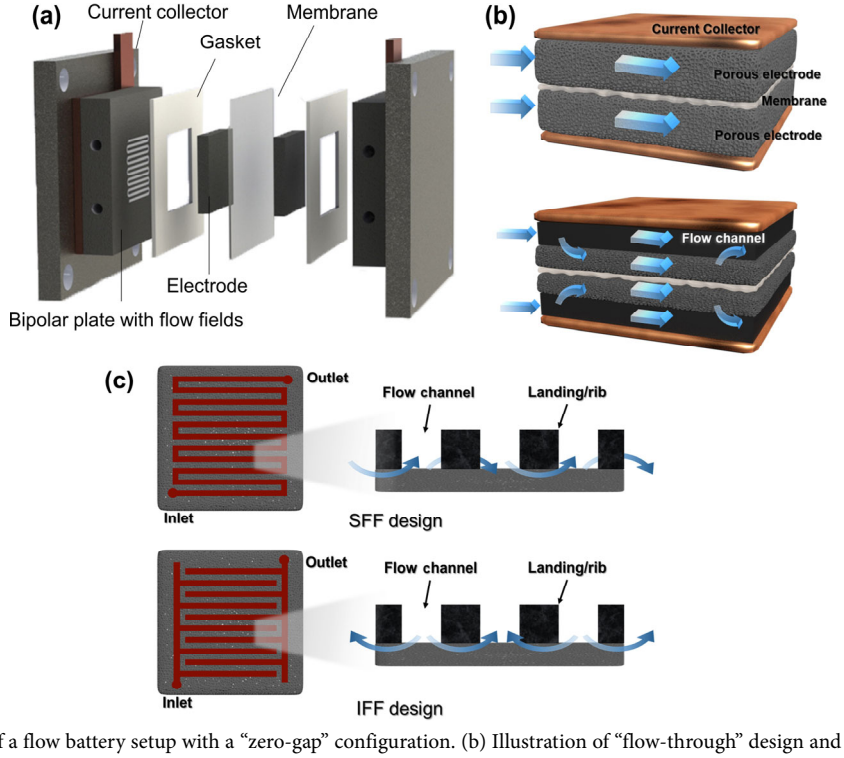


**Figure 12** (a) Schematic of a flow battery setup with a "zero-gap" configuration. (b) Illustration of "flow-through" design and "flow-by" design of porous electrodes configurations used in RFBs. (c) Serpentine flow field (SFF) design and Interdigitated flow field (IFF) design.

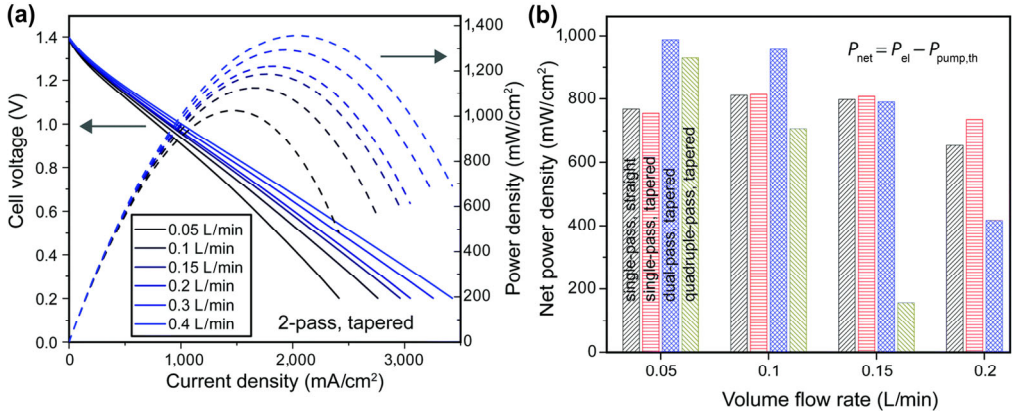


**Figure 13** (a) Cell voltage and power density vs. current density at various flow rates of the $K_4Fe(CN)_6$/2,6-DHAQ flow cell with a tapered dual-pass flow channel design. (b) Net power density determined by subtracting the theoretical pump losses from the electrical power density of the cell in (a), i.e., $P_{net} = P_{el} - P_{pump}$ vs. flow rate. Reproduced with permission from Ref. [104], © The Royal Society of Chemistry 2017.

optimizing the operating parameters prior to experimental testing.

To sum up, the advantages of optimizing the flow field and flow rate are manifold: (1) lowered ohmic loss due to the use of thinner electrodes; (2) enhanced local mass transport and minimized "dead zones" within the porous electrodes; (3) consequently improved active materials utilization and power performance. When electrolytes flow through the fluid channels and over the porous electrodes during charging and discharging, the various kinetic events such as forced convection (caused by pressure gradient), diffusion (caused by concentration gradient) and migration (caused by electric potential gradient) concurrently occur within the cell [102, 105]. Based on previous studies [106], different flow field designs may outperform each other at different operating conditions, and the deciding optimal flow design does not solely depend on the distribution of species, but on the collective roles of channel designs, electrode and electrolyte properties, and the various conditions including pressure drop and flow rate. Hence, a thorough understanding of the relationship between globalized cell performance parameters (i.e., polarizations, efficiencies, and capacities) and localized phenomena (i.e., flow homogeneity, potential and current distributions) is to be established. The integration of experimental and modelling approaches is anticipated to help expedite this process.

### 2.3 Summary

The power and energy outputs of RFBs hinge on the electrochemical properties of active redox species. The potentials of the redox species involved must be as distanced from each other as possible while with minimized side reactions to produce a high cell voltage. The fast kinetics can effectively reduce the electrochemical overpotentials and promote material utilization during battery operation. Meanwhile, a high charge concentration facilitates to reduce the concentration polarization loss at high current. Lastly, when it comes to upscaled application, the safety, stability, price, and abundance of the redox active materials should also be taken into account.

In addition to the above, battery hardware and operation conditions have profound impact on the polarizations and power performance of RFBs. Notably, hardware components also account for a major cost of cell stacks. Thus, for large-scale applications, the full potential of RFBs should be realized via innovative engineering design, as an ideal cell hardware minimizes the kinetic, ohmic, and mass transport voltage losses as well as parasitic pumping losses.

## 3 Conclusions and perspective

Because of the salient features and potentials, research into RFBs will remain prominent in the upcoming years with the rapidly growing demand for large-scale energy storage. Despite the major technological advances already achieved, the full industrialization of RFBs in both grid-scale stationary systems and distributed applications will only be accomplished when several critical challenges are adequately addressed, amongst which, high capital cost is still the primary barrier. Improving the power density and energy efficiency is an implementable and necessary approach to lower the stack sizes and thus the costs. This is particularly so for RFBs employing low-cost redox active materials. In addition to the large-scale energy storage, a reinforced power performance would broaden the applications of flow cells to other emerging areas. For instance, simultaneous heat dissipation and power delivery of an electronic device can be realized by replacing the liquid coolants with electroactive redox fluids and integrating a miniaturized flow cell stack, such as the "electronic-blood (e-Blood)" concept proposed by IBM [107]. Moreover, it has also been demonstrated that in soft robot designs, the energy density, autonomy, efficiency and multifunctionality could be boosted with the electric energy stored by redox fluids [108].

Some typical high-power RFBs at different pH values are summarized in Fig. 14 [109−112]. It can be concluded that the performance ceiling of RFBs is determined by the intrinsic properties of the employed redox mediators, including reaction kinetics, cell voltage, charge concentration, etc. This is also associated with the electrolyte environment, as clearly both the acidic and alkaline systems reveal superior power performance to the neutral ones. Meanwhile, the hardware of RFBs is also crucial in achieving a satisfactory power performance because the properties of electrode, membrane, supporting electrolyte and fluidic behavior each play a significant role in contributing to the overall polarizations during operation. Note all the reported high-power RFBs in Fig. 14 employed electrolyte flow channels, and most of them have adopted careful measures to modify the electrode and membrane. Based on the above discussion, the following are some perspectives which could be considered for the future

development of high-power, low-cost RFBs for large-scale energy storage.

(1) **Designing new redox active species through molecular engineering.** As described above, the use of organic molecules as active species has become an appealing research area due to their potentially low cost and excellent tunability in terms of redox potential, solubility, kinetics, etc., and these highly customized properties also make them suitable for RTFBs applications. Owing to the unique ability to estimate the shift of potential, solubility and stability with the changes of structure and functional groups, advanced first-principle computations, molecular dynamics simulations and machine learning are becoming more and more beneficial to the process of screening redox-active molecules. With a combination of experimental investigation with high throughput computing, the selection and optimization of redox molecules can be accelerated. Regarding the modification of redox species, compromise may have to be made between stability and redox potential. A modest potential would considerably enhance the cycling stability. In addition, synthetic methods employing low-cost and abundant precursor materials would ensure scale-up applications [113]. Some promising organic species with comparable kinetics, solubility and stability have been successfully demonstrated in ARFBs (see Fig. 15), but the degradation of organic molecules is still a persistent problem for long-term operation. Further efforts are still needed to evaluate their performance at high concentrations, and their properties at charged state would require further refinements as well.

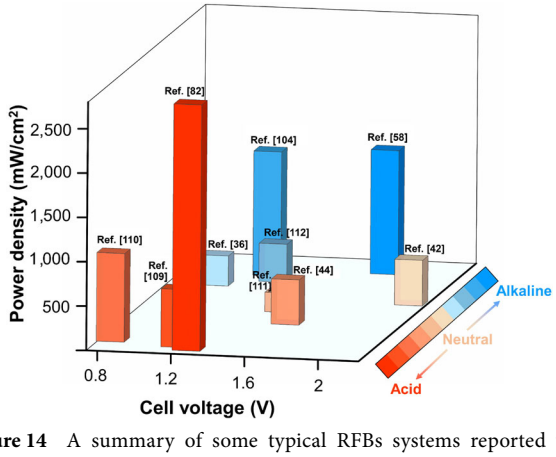


**Figure 14** A summary of some typical RFBs systems reported with high-power performance. Each column represents one case and shows the power density and cell voltage.

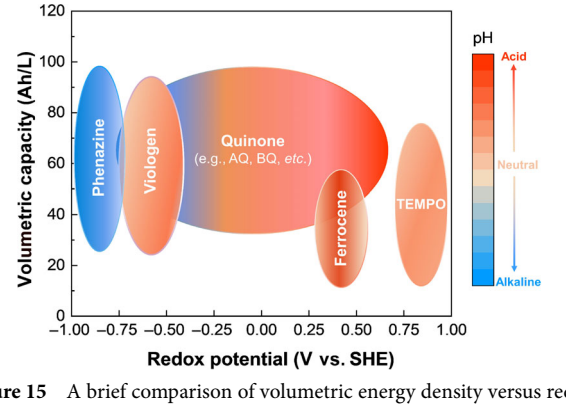


**Figure 15** A brief comparison of volumetric energy density versus redox potential for some commonly reported organic derivatives.

(2) **Development of key materials, including electrodes, membranes, supporting electrolytes and bipolar plates.** The modification and exploration of new membranes should strive to improve both ion selectivity and conductivity. Noting that the proper choice of membrane materials is an important step that can minimize the amount of time and cost spent on the optimization processes. High mechanical and chemical stability, hydrophilicity and low cost, are desirable properties for membrane materials. The PBI and SPEEEK are two promising candidates that can meet the above requirements, and some studies have shown their superior performance compared with Nafion. However, most reported advanced membranes are assigned to the conventional RFB systems, particularly VFBs. Thus, high-quality IEMs for charge carriers rather than protons, are highly desired to accelerate the development of next-generation RFBs. Specifically, the current density of pH-neutral ARFBs is marginally higher than 150 mA/cm$^2$, far behind that of VFBs (up to 600 mA/cm$^2$ or higher), with membrane acting as the main contributor of resistance within the cell [87]. Regarding the electrodes, since carbon felts are still the mainstream materials, it is essential to optimize the variables of compression ratio, pre-treatment methods, thickness, etc. before assembly and testing. Moreover, high conductivity, high mechanical strength and toughness of bipolar plates must be assured, together with well-designed flow fields embedded. Further investigations of bipolar plates used in battery stacks instead of a single cell are necessary to elevate the power outputs of the large-scale battery systems. Meanwhile, there is also an urgent demand to develop an affordable industrial method for the mass production of bipolar plates with customized flow channels.

(3) **Employment of computational simulation and *in-situ* characterization for RFB systems.** Computation and modelling of RFBs have generally trailed to the development of experimental and demonstration progress. However, mathematical modeling and simulation are essential to fully understand the various fluid mechanics, physiochemical phenomena and current distributions involved in RFBs. Through simulation, there has been major progress in qualitatively understanding how each individual variable affects the power performance. In addition, when combining with the experimental techniques, for example, the utilization of internal sensors or *in-situ* probes to monitor the localized phenomena [114–116], the mathematical models can be fine-tuned to be more accurate and precise, which contributes to the determination and refinement of limiting parameters. Regretfully, there is still a lack of mathematical or physical models to evaluate the overall impact of different kinetics events together, which is, however, quite necessary to identify the dominant limiting factor in a complicated configuration. Besides, most research on RFB simulation remains at the stage of the mass transport within a single cell. Nonetheless, multi-scale modeling from the interactions of redox species, up to the operation of battery stack at system level, is an area well worth studying.

(4) **Engineering optimization and management of stack system.** The majority of academic studies have been focused on the exhibition of a small single cell, but these short-term laboratory results are not necessarily realistic for advancing the RFBs technology for practical operations. Although a large number of patents have been filed [102], the lack of evidence for the durability, reliability and stability of scaleup manifestation, critically hinders the confidence of rolling out and wider deployment [105]. As some of the laboratory single cells have

already presented attractive power performance, the "last-mile problem" for the commercialization of RFBs is a scale-up demonstration of the system while maintaining its performance as much as possible. Moving forward, more attention should be spent on engineering aspects, such as full-size stacks design, installation, as well as automated control systems to operate RFBs safely and maximize the stack performance. Additionally, practical strategies are also required to solve the issues from devices, such as electrical shunt loss, electrolyte leakage and corrosion, severe water immigration, component aging and degradation, etc.

In this review, we have examined the foremost intrinsic and extrinsic factors directly associated with the power performance of RFBs and proposed some implementable strategies to improve each aspect. With the judicious integration of fundamental, applied and translational research, it is anticipated that RFBs technologies, with their unique strengths, will satisfy the requirements of industrial utilization and gain an entrance to the vast market of stationary energy storage.

## Acknowledgements

This research is supported by the National Research Foundation, Prime Minister's Office, Singapore under its Investigatorship Programme (Award No. NRF-NRFI2018-06).

## Declaration of conflicting interests

The authors declare no conflicting interests regarding the content of this article.

## References

[1] Van Soest, H. L.; Den Elzen, M. G. J.; Van Vuuren, D. P. Net-zero emission targets for major emitting countries consistent with the Paris Agreement. *Nat. Commun.* **2021**, *12*, 2140.

[2] Bird, L.; Lew, D.; Milligan, M.; Carlini, E. M.; Estanqueiro, A.; Flynn, D.; Gomez-Lazaro, E.; Holttinen, H.; Menemenlis, N.; Orths, A. et al. Wind and solar energy curtailment: A review of international experience. *Renewable Sustainable Energy Rev.* **2016**, *65*, 577–586.

[3] Luo, J.; Hu, B.; Hu, M. W.; Zhao, Y.; Liu, T. L. Status and prospects of organic redox flow batteries toward sustainable energy storage. *ACS Energy Lett.* **2019**, *4*, 2220–2240.

[4] Aneke, M.; Wang, M. H. Energy storage technologies and real life applications-a state of the art review. *Appl. Energy* **2016**, *179*, 350–377.

[5] Chen, Y. Q.; Kang, Y. Q.; Zhao, Y.; Wang, L.; Liu, J. L.; Li, Y. X.; Liang, Z.; He, X. M.; Li, X.; Tavajohi, N. et al. A review of lithium-ion battery safety concerns: The issues, strategies, and testing standards. *J. Energy Chem.* **2021**, *59*, 83–99.

[6] Park, M.; Ryu, J.; Wang, W.; Cho, J. Material design and engineering of next-generation flow-battery technologies. *Nat. Rev. Mater.* **2017**, *2*, 16080.

[7] Sánchez-Díez, E.; Ventosa, E.; Guarnieri, M.; Trovò, A.; Flox, C.; Marcilla, R.; Soavi, F.; Mazur, P.; Aranzabe, E.; Ferret, R. Redox flow batteries: Status and perspective towards sustainable stationary energy storage. *J. Power Sources* **2021**, *481*, 228804.

[8] Mohamed, M. R.; Sharkh, S. M.; Walsh, F. C. Redox flow batteries for hybrid electric vehicles: Progress and challenges. In *2009 IEEE Vehicle Power and Propulsion Conference*, Dearborn, USA, 2009, pp 551–557.

[9] Yao, Y. X.; Lei, J. F.; Shi, Y.; Ai, F.; Lu, Y. C. Assessment methods and performance metrics for redox flow batteries. *Nat. Energy* **2021**, *6*, 582–588.

[10] Li, T. Y.; Xing, F.; Liu, T.; Sun, J. W.; Shi, D. Q.; Zhang, H. M.; Li, X. F. Cost, performance prediction and optimization of a vanadium flow battery by machine-learning. *Energy Environ. Sci.* **2020**, *13*, 4353–4361.

[11] Viswanathan, V.; Crawford, A.; Thaller, L.; Stephenson, D.; Kim, S.; Wang, W.; Coffey, G.; Balducci, P.; Gary, Z.; Yang, L. L. Estimation of capital and levelized cost for redox flow batteries. *US Department of Energy* (*USDOE-OE ESS*), *Peer Review at Washington, DC* **2012**.

[12] Chalamala, B. R.; Soundappan, T.; Fisher, G. R.; Anstey, M. R.; Viswanathan, V. V.; Perry, M. L. Redox flow batteries: An engineering perspective. *Proc. IEEE* **2014**, *102*, 976–999.

[13] Perry, M. L.; Darling, R. M.; Zaffou, R. High power density redox flow battery cells. *ECS Trans.* **2013**, *53*, 7–16.

[14] Lu, W. J.; Li, X. F.; Zhang, H. M. The next generation vanadium flow batteries with high power density-a perspective. *Phys. Chem. Chem. Phys.* **2018**, *20*, 23–35.

[15] Skyllas-Kazacos, M.; Chakrabarti, M. H.; Hajimolana, S. A.; Mjalli, F. S.; Saleem, M. Progress in flow battery research and development. *J. Electrochem. Soc.* **2011**, *158*, R55.

[16] Andreev, A. A.; Sridhar, A.; Sabry, M. M.; Zapater, M.; Ruch, P.; Michel, B.; Atienza, D. PowerCool: Simulation of cooling and powering of 3D MPSoCs with integrated flow cell arrays. *IEEE Trans. Comput.* **2018**, *67*, 73–85.

[17] Bard, A. J.; Faulkner, L. R.; White, H. S. *Electrochemical Methods: Fundamentals and Applications*; John Wiley & Sons: Hoboken, 2022.

[18] Aaron, D.; Tang, Z. J.; Papandrew, A. B.; Zawodzinski, T. A. Polarization curve analysis of all-vanadium redox flow batteries. *J. Appl. Electrochem.* **2011**, *41*, 1175–1182.

[19] Emmett, R. K.; Roberts, M. E. Recent developments in alternative aqueous redox flow batteries for grid-scale energy storage. *J. Power Sources* **2021**, *506*, 230087.

[20] Arévalo-Cid, P.; Dias, P.; Mendes, A.; Azevedo, J. Redox flow batteries: A new frontier on energy storage. *Sustainable Energy Fuels* **2021**, *5*, 5366–5419.

[21] Hofmann, J. D.; Schröder, D. Which parameter is governing for aqueous redox flow batteries with organic active material? *Chem. Ing. Tech.* **2019**, *91*, 786–794.

[22] Wang, H.; Sayed, S. Y.; Luber, E. J.; Olsen, B. C.; Shirurkar, S. M.; Venkatakrishnan, S.; Tefashe, U. M.; Farquhar, A. K.; Smotkin, E. S.; McCreery, R. L. et al. Redox flow batteries: How to determine electrochemical kinetic parameters. *ACS Nano* **2020**, *14*, 2575–2584.

[23] Chen, P.; Fryling, M. A.; McCreery, R. L. Electron transfer kinetics at modified carbon electrode surfaces: The role of specific surface sites. *Anal. Chem.* **1995**, *67*, 3115–3122.

[24] Weber, A. Z.; Mench, M. M.; Meyers, J. P.; Ross, P. N.; Gostick, J. T.; Liu, Q. H. Redox flow batteries: A review. *J. Appl. Electrochem.* **2011**, *41*, 1137–1164.

[25] Fink, H.; Friedl, J.; Stimming, U. Composition of the electrode determines which half-cell's rate constant is higher in a vanadium flow battery. *J. Phys. Chem. C* **2016**, *120*, 15893–15901.

[26] Chen, Q. R.; Lv, Y. G.; Yuan, Z. Z.; Li, X. F.; Yu, G. H.; Yang, Z. J.; Xu, T. W. Organic electrolytes for pH-neutral aqueous organic redox flow batteries. *Adv. Funct. Mater.* **2022**, *32*, 2108777.

[27] Luo, J.; Sam, A.; Hu, B.; DeBruler, C.; Wei, X. L.; Wang, W.; Liu, T. L. Unraveling pH dependent cycling stability of ferricyanide/ferrocyanide in redox flow batteries. *Nano Energy* **2017**, *42*, 215–221.

[28] Roznyatovskaya, N.; Noack, J.; Pinkwart, K.; Tübke, J. Aspects of electron transfer processes in vanadium redox-flow batteries. *Curr. Opin. Electrochem.* **2020**, *19*, 42–48.

[29] Park, M.; Ryu, J.; Cho, J. Nanostructured electrocatalysts for all-vanadium redox flow batteries. *Chem. Asian J.* **2015**, *10*, 2096–2110.

[30] Singh, M. K.; Kapoor, M.; Verma, A. Recent progress on carbon and metal based electrocatalysts for vanadium redox flow battery. *WIRs Energy Environ.* **2021**, *10*, e393.

[31] Li, B.; Gu, M.; Nie, Z. M.; Shao, Y. Y.; Luo, Q. T.; Wei, X. L.; Li, X. L.; Xiao, J.; Wang, C. M.; Sprenkle, V. et al. Bismuth nanoparticle decorating graphite felt as a high-performance electrode for an all-vanadium redox flow battery. *Nano Lett.* **2013**, *13*, 1330–1335.

[32] Zhang, F. F.; Huang, S. P.; Wang, X.; Jia, C. K.; Du, Y. H.; Wang, Q. Redox-targeted catalysis for vanadium redox-flow batteries. *Nano Energy* **2018**, *52*, 292–299.

[33] Ma, D.; Hu, B.; Wu, W. D.; Liu, X.; Zai, J. T.; Shu, C.; Tadesse Tsega, T.; Chen, L. W.; Qian, X. F.; Liu, T. L. Highly active nanostructured $CoS_2$/CoS heterojunction electrocatalysts for aqueous polysulfide/iodide redox flow batteries. *Nat. Commun.* **2019**, *10*, 3367.
[34] Gao, M. Q.; Huang, S. P.; Zhang, F. F.; Lee, Y. M.; Huang, S. Q.; Wang, Q. Successive ionic layer adsorption and reaction-deposited copper sulfide electrocatalyst for high-power polysulfide-based aqueous flow batteries. *Mater. Today Energy* **2020**, *18*, 100540.
[35] Liu, Y. H.; Li, Y. Y.; Zuo, P. P.; Chen, Q. R.; Tang, G. G.; Sun, P.; Yang, Z. J.; Xu, T. W. Screening viologen derivatives for neutral aqueous organic redox flow batteries. *ChemSusChem* **2020**, *13*, 2245–2249.
[36] Wu, M.; Jing, Y.; Wong, A. A.; Fell, E. M.; Jin, S. J.; Tang, Z. J.; Gordon, R. G.; Aziz, M. J. Extremely stable anthraquinone negolytes synthesized from common precursors. *Chem* **2020**, *6*, 1432–1442.
[37] Amini, K.; Gostick, J.; Pritzker, M. D. Metal and metal oxide electrocatalysts for redox flow batteries. *Adv. Funct. Mater.* **2020**, *30*, 1910564.
[38] Choi, C.; Kim, S.; Kim, R.; Choi, Y.; Kim, S.; Jung, H. Y.; Yang, J. H.; Kim, H. T. A review of vanadium electrolytes for vanadium redox flow batteries. *Renewable Sustainable Energy Rev.* **2017**, *69*, 263–274.
[39] Chao, D. L.; Qiao, S. Z. Toward high-voltage aqueous batteries: Super- or low-concentrated electrolyte? *Joule* **2020**, *4*, 1846–1851.
[40] Wang, X.; Gao, M. Q.; Lee, Y. M.; Salla, M.; Zhang, F. F.; Huang, S. P.; Wang, Q. E-blood: High power aqueous redox flow cell for concurrent powering and cooling of electronic devices. *Nano Energy* **2022**, *93*, 106864.
[41] Liu, Z. X.; Huang, Y.; Huang, Y.; Yang, Q.; Li, X. L.; Huang, Z. D.; Zhi, C. Y. Voltage issue of aqueous rechargeable metal-ion batteries. *Chem. Soc. Rev.* **2020**, *49*, 180–232.
[42] Robb, B. H.; Farrell, J. M.; Marshak, M. P. Chelated chromium electrolyte enabling high-voltage aqueous flow batteries. *Joule* **2019**, *3*, 2503–2512.
[43] Liu, Y.; Dai, G. L.; Chen, Y. Y.; Wang, R.; Li, H. M.; Shi, X. L.; Zhang, X. H.; Xu, Y.; Zhao, Y. Effective design strategy of small bipolar molecules through fused conjugation toward 2.5 V based redox flow batteries. *ACS Energy Lett.* **2022**, *7*, 1274–1283.
[44] Gao, M. Q.; Salla, M.; Song, Y. X.; Wang, Q. High-power near-neutral aqueous all organic redox flow battery enabled with a pair of anionic redox species. *Angew. Chem., Int. Ed.* **2022**, *61*, e202208223.
[45] Gu, S.; Gong, K.; Yan, E. Z.; Yan, Y. S. A multiple ion-exchange membrane design for redox flow batteries. *Energy Environ. Sci.* **2014**, *7*, 2986–2998.
[46] Zhong, C.; Liu, B.; Ding, J.; Liu, X. R.; Zhong, Y. W.; Li, Y.; Sun, C. B.; Han, X. P.; Deng, Y. D.; Zhao, N. Q. et al. Decoupling electrolytes towards stable and high-energy rechargeable aqueous zinc-manganese dioxide batteries. *Nat. Energy* **2020**, *5*, 440–449.
[47] Yu, V. K.; Chen, D. Peak power prediction of a vanadium redox flow battery. *J. Power Sources* **2014**, *268*, 261–268.
[48] Li, Z. J.; Weng, G. M.; Zou, Q. L.; Cong, G. T.; Lu, Y. C. A high-energy and low-cost polysulfide/iodide redox flow battery. *Nano Energy* **2016**, *30*, 283–292.
[49] Ding, Y.; Zhang, C. K.; Zhang, L. Y.; Zhou, Y. G.; Yu, G. H. Molecular engineering of organic electroactive materials for redox flow batteries. *Chem. Soc. Rev.* **2018**, *47*, 69–103.
[50] Hu, B.; DeBruler, C.; Rhodes, Z.; Liu, T. L. Long-cycling aqueous organic redox flow battery (AORFB) toward sustainable and safe energy storage. *J. Am. Chem. Soc.* **2017**, *139*, 1207–1214.
[51] Yu, J. Z.; Salla, M.; Zhang, H.; Ji, Y.; Zhang, F. F.; Zhou, M. Y.; Wang, Q. A robust anionic sulfonated ferrocene derivative for pH-neutral aqueous flow battery. *Energy Storage Mater.* **2020**, *29*, 216–222.
[52] Jin, S. J.; Jing, Y.; Kwabi, D. G.; Ji, Y. L.; Tong, L.; De Porcellinis, D.; Goulet, M. A.; Pollack, D. A.; Gordon, R. G.; Aziz, M. J. A water-miscible quinone flow battery with high volumetric capacity and energy density. *ACS Energy Lett.* **2019**, *4*, 1342–1348.
[53] Zhang, C. K.; Chen, H.; Qian, Y. M.; Dai, G. L.; Zhao, Y.; Yu, G. H. General design methodology for organic eutectic electrolytes toward high-energy-density redox flow batteries. *Adv. Mater.* **2021**, *33*, 2008560.
[54] Zhang, C. K.; Qian, Y. M.; Ding, Y.; Zhang, L. Y.; Guo, X. L.; Zhao, Y.; Yu, G. H. Biredox eutectic electrolytes derived from organic redox-active molecules: High-energy storage systems. *Angew. Chem., Int. Ed.* **2019**, *58*, 7045–7050.
[55] Shi, Y.; Wang, Z. Y.; Yao, Y. X.; Wang, W. W.; Lu, Y. C. High-areal-capacity conversion type iron-based hybrid redox flow batteries. *Energy Environ. Sci.* **2021**, *14*, 6329–6337.
[56] Khor, A.; Leung, P.; Mohamed, M. R.; Flox, C.; Xu, Q.; An, L.; Wills, R. G. A.; Morante, J. R.; Shah, A. A. Review of zinc-based hybrid flow batteries: From fundamentals to applications. *Mater. Today Energy* **2018**, *8*, 80–108.
[57] Yuan, Z. Z.; Yin, Y. B.; Xie, C. X.; Zhang, H. M.; Yao, Y.; Li, X. F. Advanced materials for zinc-based flow battery: Development and challenge. *Adv. Mater.* **2019**, *31*, 1902025.
[58] Yuan, Z. Z.; Liang, L. X.; Dai, Q.; Li, T. Y.; Song, Q. L.; Zhang, H. M.; Hou, G. J.; Li, X. F. Low-cost hydrocarbon membrane enables commercial-scale flow batteries for long-duration energy storage. *Joule* **2022**, *6*, 884–905.
[59] Wang, G. X.; Zou, H. T.; Zhu, X. B.; Ding, M.; Jia, C. K. Recent progress in zinc-based redox flow batteries: A review. *J. Phys. D: Appl. Phys.* **2022**, *55*, 163001.
[60] Duduta, M.; Ho, B.; Wood, V. C.; Limthongkul, P.; Brunini, V. E.; Carter, W. C.; Chiang, Y. M. Semi-solid lithium rechargeable flow battery. *Adv. Energy Mater.* **2011**, *1*, 511–516.
[61] Ventosa, E. Semi-solid flow battery and redox-mediated flow battery: Two strategies to implement the use of solid electroactive materials in high-energy redox-flow batteries. *Curr. Opin. Chem. Eng.* **2022**, *37*, 100834.
[62] Huang, Q. Z.; Wang, Q. Next-generation, high-energy-density redox flow batteries. *ChemPlusChem* **2015**, *80*, 312–322.
[63] Yan, R. T.; Wang, Q. Redox-targeting-based flow batteries for large-scale energy storage. *Adv. Mater.* **2018**, *30*, 1802406.
[64] Zhou, M. Y.; Chen, Y.; Salla, M.; Zhang, H.; Wang, X.; Mothe, S. R.; Wang, Q. Single-molecule redox-targeting reactions for a pH-neutral aqueous organic redox flow battery. *Angew. Chem., Int. Ed.* **2020**, *59*, 14286–14291.
[65] Zhang, F. F.; Gao, M. Q.; Huang, S. Q.; Zhang, H.; Wang, X.; Liu, L. J.; Han, M.; Wang, Q. Redox targeting of energy materials for energy storage and conversion. *Adv. Mater.* **2022**, *34*, 2104562.
[66] Chen, Y.; Zhou, M. Y.; Xia, Y. H.; Wang, X.; Liu, Y.; Yao, Y.; Zhang, H.; Li, Y.; Lu, S. T.; Qin, W. et al. A stable and high-capacity redox targeting-based electrolyte for aqueous flow batteries. *Joule* **2019**, *3*, 2255–2267.
[67] Cheng, Y. H.; Wang, X.; Huang, S. P.; Samarakoon, W.; Xi, S. B.; Ji, Y.; Zhang, H.; Zhang, F. F.; Du, Y. H.; Feng, Z. X. et al. Redox targeting-based vanadium redox-flow battery. *ACS Energy Lett.* **2019**, *4*, 3028–3035.
[68] Noack, J.; Roznyatovskaya, N.; Herr, T.; Fischer, P. The chemistry of redox-flow batteries. *Angew. Chem., Int. Ed.* **2015**, *54*, 9776–9809.
[69] Jiang, L. W.; Dong, D. J.; Lu, Y. C. Design strategies for low temperature aqueous electrolytes. *Nano Res. Energy* **2022**, *1*, e9120003.
[70] Leung, P.; Li, X. H.; De León, C. P.; Berlouis, L.; Low, C. T. J.; Walsh, F. C. Progress in redox flow batteries, remaining challenges and their applications in energy storage. *RSC Adv.* **2012**, *2*, 10125–10156.
[71] Chakrabarti, M. H.; Brandon, N. P.; Hajimolana, S. A.; Tariq, F.; Yufit, V.; Hashim, M. A.; Hussain, M. A.; Low, C. T. J.; Aravind, P. V. Application of carbon materials in redox flow batteries. *J. Power Sources* **2014**, *253*, 150–166.
[72] Ye, R. J.; Henkensmeier, D.; Yoon, S. J.; Huang, Z. F.; Kim, D. K.; Chang, Z. J.; Kim, S.; Chen, R. Y. Redox flow batteries for energy storage: A technology review. *J. Electrochem. Energy Convers. Storage* **2018**, *15*, 010801.
[73] Wang, R.; Li, Y. S. Carbon electrodes improving electrochemical activity and enhancing mass and charge transports in aqueous flow

battery: Status and perspective. *Energy Storage Mater*. **2020**, *31*, 230–251.

[74] Shao, Y. Y.; Wang, X. Q.; Engelhard, M.; Wang, C. M.; Dai, S.; Liu, J.; Yang, Z. G.; Lin, Y. H. Nitrogen-doped mesoporous carbon for energy storage in vanadium redox flow batteries. *J. Power Sources* **2010**, *195*, 4375–4379.

[75] Wu, L. T.; Shen, Y.; Yu, L. H.; Xi, J. Y.; Qiu, X. P. Boosting vanadium flow battery performance by nitrogen-doped carbon nanospheres electrocatalyst. *Nano Energy* **2016**, *28*, 19–28.

[76] Miller, M. A.; Bourke, A.; Quill, N.; Wainright, J. S.; Lynch, R. P.; Buckley, D. N.; Savinell, R. F. Kinetic study of electrochemical treatment of carbon fiber microelectrodes leading to *in situ* enhancement of vanadium flow battery efficiency. *J. Electrochem. Soc*. **2016**, *163*, A2095–A2102.

[77] Banerjee, R.; Bevilacqua, N.; Mohseninia, A.; Wiedemann, B.; Wilhelm, F.; Scholta, J.; Zeis, R. Carbon felt electrodes for redox flow battery: Impact of compression on transport properties. *J. Energy Storage* **2019**, *26*, 100997.

[78] Park, S. K.; Shim, J.; Yang, J. H.; Jin, C. S.; Lee, B. S.; Lee, Y. S.; Shin, K. H.; Jeon, J. D. The influence of compressed carbon felt electrodes on the performance of a vanadium redox flow battery. *Electrochim. Acta* **2014**, *116*, 447–452.

[79] Gundlapalli, R.; Jayanti, S. Effect of electrode compression and operating parameters on the performance of large vanadium redox flow battery cells. *J. Power Sources* **2019**, *427*, 231–242.

[80] Zhou, X. L.; Zeng, Y. K.; Zhu, X. B.; Wei, L.; Zhao, T. S. A high-performance dual-scale porous electrode for vanadium redox flow batteries. *J. Power Sources* **2016**, *325*, 329–336.

[81] Aaron, D. S.; Liu, Q.; Tang, Z.; Grim, G. M.; Papandrew, A. B.; Turhan, A.; Zawodzinski, T. A.; Mench, M. M. Dramatic performance gains in vanadium redox flow batteries through modified cell architecture. *J. Power Sources* **2012**, *206*, 450–453.

[82] Jiang, H. R.; Sun, J.; Wei, L.; Wu, M. C.; Shyy, W.; Zhao, T. S. A high power density and long cycle life vanadium redox flow battery. *Energy Storage Mater*. **2020**, *24*, 529–540.

[83] Zeng, L.; Zhao, T. S.; Wei, L.; Jiang, H. R.; Wu, M. C. Anion exchange membranes for aqueous acid-based redox flow batteries: Current status and challenges. *Appl. Energy* **2019**, *233–234*, 622–643.

[84] Hickner, M. A.; Herring, A. M.; Coughlin, E. B. Anion exchange membranes: Current status and moving forward. *J. Polym. Sci. Part B Polym. Phys*. **2013**, *51*, 1727–1735.

[85] Jin, S. J.; Fell, E. M.; Vina-Lopez, L.; Jing, Y.; Michalak, P. W.; Gordon, R. G.; Aziz, M. J. Near neutral pH redox flow battery with low permeability and long-lifetime phosphonated viologen active species. *Adv. Energy Mater*. **2020**, *10*, 2000100.

[86] Yuan, Z. Z.; Zhang, H. M.; Li, X. F. Ion conducting membranes for aqueous flow battery systems. *Chem. Commun*. **2018**, *54*, 7570–7588.

[87] Xiong, P.; Zhang, L. Y.; Chen, Y. Y.; Peng, S. S.; Yu, G. H. A chemistry and microstructure perspective on ion-conducting membranes for redox flow batteries. *Angew. Chem., Int. Ed*. **2021**, *60*, 24770–24798.

[88] Lee, K. J.; Chu, Y. H. Preparation of the graphene oxide (GO)/Nafion composite membrane for the vanadium redox flow battery (VRB) system. *Vacuum* **2014**, *107*, 269–276.

[89] Xi, J. Y.; Wu, Z. H.; Qiu, X. P.; Chen, L. Q. Nafion/$SiO_2$ hybrid membrane for vanadium redox flow battery. *J. Power Sources* **2007**, *166*, 531–536.

[90] Teng, X. G.; Zhao, Y. T.; Xi, J. Y.; Wu, Z. H.; Qiu, X. P.; Chen, L. Q. Nafion/organic silica modified $TiO_2$ composite membrane for vanadium redox flow battery via *in situ* sol-gel reactions. *J. Membr. Sci*. **2009**, *341*, 149–154.

[91] Mai, Z.; Zhang, H. M.; Li, X. F.; Xiao, S. H.; Zhang, H. Z. Nafion/polyvinylidene fluoride blend membranes with improved ion selectivity for vanadium redox flow battery application. *J. Power Sources* **2011**, *196*, 5737–5741.

[92] Kuwertz, R.; Kirstein, C.; Turek, T.; Kunz, U. Influence of acid pretreatment on ionic conductivity of Nafion® membranes. *J. Membr. Sci*. **2016**, *500*, 225–235.

[93] Schwenzer, B.; Zhang, J. L.; Kim, S.; Li, L. Y.; Liu, J.; Yang, Z. G. Membrane development for vanadium redox flow batteries. *ChemSusChem* **2011**, *4*, 1388–1406.

[94] Li, Z. J.; Lu, Y. C. Polysulfide-based redox flow batteries with long life and low levelized cost enabled by charge-reinforced ion-selective membranes. *Nat. Energy* **2021**, *6*, 517–528.

[95] Chen, D. J.; Qi, H. N.; Sun, T. T.; Yan, C.; He, Y. Y.; Kang, C. Z.; Yuan, Z. Z.; Li, X. F. Polybenzimidazole membrane with dual proton transport channels for vanadium flow battery applications. *J. Membr. Sci*. **2019**, *586*, 202–210.

[96] Yuan, Z. Z.; Liu, X. Q.; Xu, W. B.; Duan, Y. Q.; Zhang, H. M.; Li, X. F. Negatively charged nanoporous membrane for a dendrite-free alkaline zinc-based flow battery with long cycle life. *Nat. Commun*. **2018**, *9*, 3731.

[97] Gao, M. Q.; Salla, M.; Zhang, F. F.; Zhi, Y. F.; Wang, Q. Membrane fouling in aqueous redox flow batteries. *J. Power Sources* **2022**, *527*, 231180.

[98] Pourcelly, G.; Oikonomou, A.; Gavach, C.; Hurwitz, H. D. Influence of the water content on the kinetics of counter-ion transport in perfluorosulphonic membranes. *J. Electroanal. Chem. Interfacial Electrochem*. **1990**, *287*, 43–59.

[99] Stenina, I. A.; Sistat, P.; Rebrov, A. I.; Pourcelly, G.; Yaroslavtsev, A. B. Ion mobility in Nafion-117 membranes. *Desalination* **2004**, *170*, 49–57.

[100] Wessells, C.; Ruffo, R.; Huggins, R. A.; Cui, Y. Investigations of the electrochemical stability of aqueous electrolytes for lithium battery applications. *Electrochem. Solid-State Lett*. **2010**, *13*, A59.

[101] Suo, L. M.; Borodin, O.; Gao, T.; Olguin, M.; Ho, J.; Fan, X. L.; Luo, C.; Wang, C. S.; Xu, K. "Water-in-salt" electrolyte enables high-voltage aqueous lithium-ion chemistries. *Science* **2015**, *350*, 938–943.

[102] Ke, X. Y.; Prahl, J. M.; Alexander, J. I. D.; Wainright, J. S.; Zawodzinski, T. A.; Savinell, R. F. Rechargeable redox flow batteries: Flow fields, stacks and design considerations. *Chem. Soc. Rev*. **2018**, *47*, 8721–8743.

[103] Elgammal, R. A.; Tang, Z. J.; Sun, C. N.; Lawton, J.; Zawodzinski, Jr. T. A. Species uptake and mass transport in membranes for vanadium redox flow batteries. *Electrochim. Acta* **2017**, *237*, 1–11.

[104] Marschewski, J.; Brenner, L.; Ebejer, N.; Ruch, P.; Michel, B.; Poulikakos, D. 3D-printed fluidic networks for high-power-density heat-managing miniaturized redox flow batteries. *Energy Environ. Sci*. **2017**, *10*, 780–787.

[105] Arenas, L. F.; De León, C. P.; Walsh, F. C. Redox flow batteries for energy storage: Their promise, achievements and challenges. *Curr. Opin. Electrochem*. **2019**, *16*, 117–126.

[106] Esan, O. C.; Shi, X. Y.; Pan, Z. F.; Huo, X. Y.; An, L.; Zhao, T. S. Modeling and simulation of flow batteries. *Adv. Energy Mater*. **2020**, *10*, 2000758.

[107] Ruch, P.; Brunschwiler, T.; Escher, W.; Paredes, S.; Michel, B. Toward five-dimensional scaling: How density improves efficiency in future computers. *IBM J. Res. Dev*. **2011**, *55*, 15:1–15:13.

[108] Aubin, C. A.; Choudhury, S.; Jerch, R.; Archer, L. A.; Pikul, J. H.; Shepherd, R. F. Electrolytic vascular systems for energy-dense robots. *Nature* **2019**, *571*, 51–57.

[109] Zeng, Y. K.; Zhou, X. L.; Zeng, L.; Yan, X. H.; Zhao, T. S. Performance enhancement of iron-chromium redox flow batteries by employing interdigitated flow fields. *J. Power Sources* **2016**, *327*, 258–264.

[110] Chen, Q.; Gerhardt, M. R.; Hartle, L.; Aziz, M. J. A quinone-bromide flow battery with 1 W/$cm^2$ power density. *J. Electrochem. Soc*. **2016**, *163*, A5010–A2013.

[111] Luo, J.; Wu, W. D.; Debruler, C.; Hu, B.; Hu, M. W.; Liu, T. L. A 1.51 V pH neutral redox flow battery towards scalable energy storage. *J. Mater. Chem. A* **2019**, *7*, 9130–9136.

[112] Wang, C. X.; Li, X.; Yu, B.; Wang, Y. R.; Yang, Z.; Wang, H. Z.; Lin, H. N.; Ma, J.; Li, G. G.; Jin, Z. Molecular design of fused-ring phenazine derivatives for long-cycling alkaline redox flow batteries. *ACS Energy Lett*. **2020**, *5*, 411–417.

[113] Lv, X. L.; Sullivan, P.; Fu, H. C.; Hu, X. X.; Liu, H. H.; Jin, S.; Li, W. J.; Feng, D. W. Dextrosil-viologen: A robust and sustainable anolyte for aqueous organic redox flow batteries. *ACS Energy Lett*. **2022**, *7*, 2428–2434.
[114] Becker, M.; Bredemeyer, N.; Tenhumberg, N.; Turek, T. Polarization curve measurements combined with potential probe sensing for determining current density distribution in vanadium redox-flow batteries. *J. Power Sources* **2016**, *307*, 826–833.
[115] Zhou, M. Y.; Huang, Q. Z.; Truong, T. N. P.; Ghilane, J.; Zhu, Y. G.; Jia, C. K.; Yan, R. T.; Fan, L.; Randriamahazaka, H.; Wang, Q. Nernstian-potential-driven redox-targeting reactions of battery materials. *Chem* **2017**, *3*, 1036–1049.
[116] Jing, Y.; Zhao, E. W.; Goulet, M. A.; Bahari, M.; Fell, E. M.; Jin, S. J.; Davoodi, A.; Jónsson, E.; Wu, M.; Grey, C. P. et al. *In situ* electrochemical recomposition of decomposed redox-active species in aqueous organic flow batteries. *Nat. Chem*. **2022**, *14*, 1103–1109.

**Mengqi GAO** is currently a Ph.D. candidate in the Department of Materials Science and Engineering, National University of Singapore. He received his Bachelor of Science degree in Chemistry from University of Chinese Academy of Sciences in 2018. His research interest includes the development of active materials and devices for high-power density aqueous redox flow batteries.

**Qing WANG** is currently a Dean's Chair Associate Professor at the Department of Materials Science and Engineering, National University of Singapore. He obtained his Ph.D. in physics at the Institute of Physics, Chinese Academy of Sciences in 2002. He leads a research group on the fundamental understanding of charge transport/transfer in mesoscopic electrochemical systems and their applications for advanced energy conversion and storage, including the redox targeting-based flow batteries and beyond, with the implementations to a wide variety of battery chemistries and energy materials for advanced energy conversion and storage.